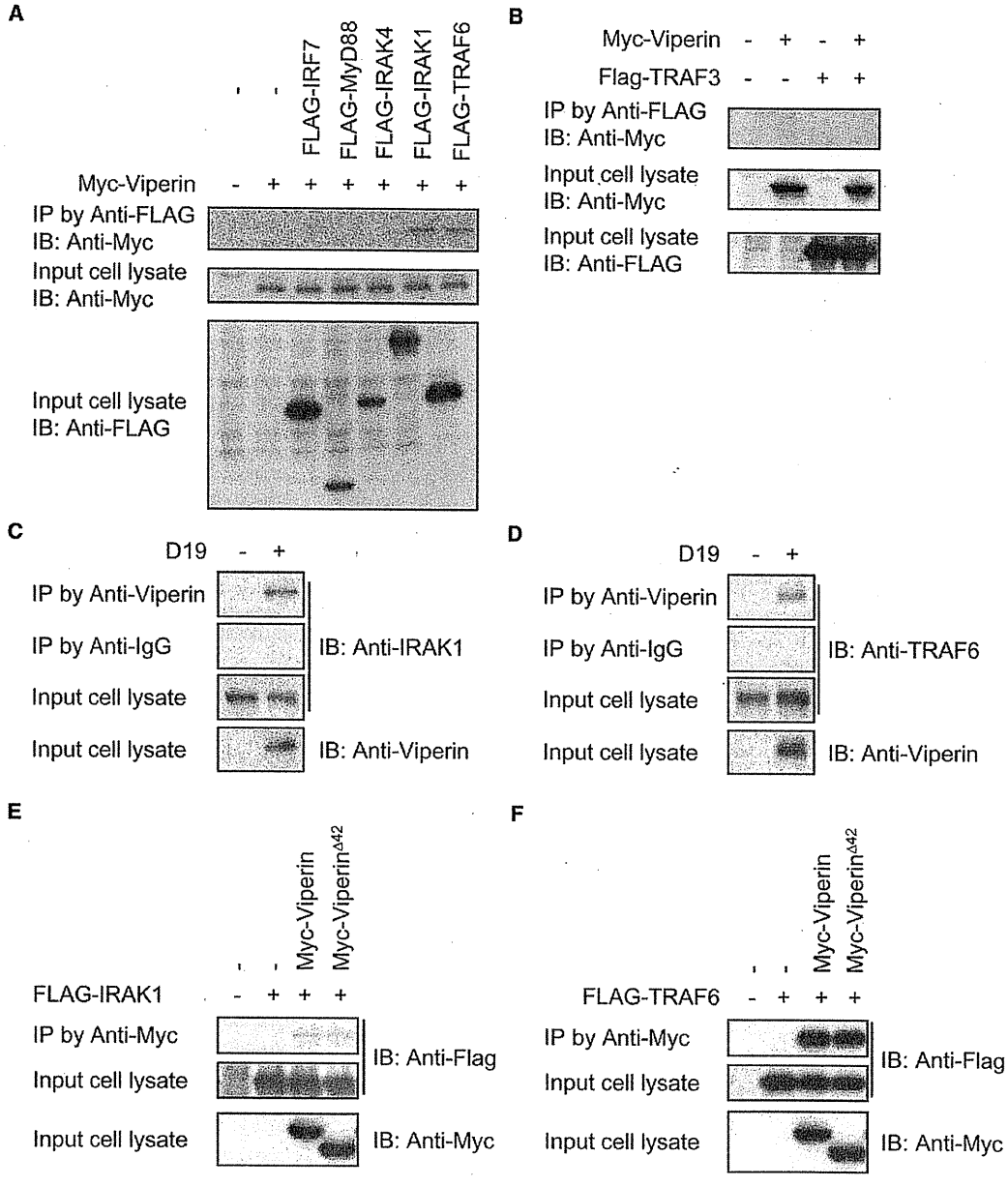

Figure 3. Viperin Interacts with IRAK1 and TRAF6

(A and B) 293 cells were transfected with the indicated expression plasmids. Whole-cell lysate was subjected to immunoprecipitation coupled with immunoblotting analysis.

(C and D) FLT3L-induced bone marrow dendritic cells isolated from C57/BL6 mice were stimulated with D19 (1 μM) for 5 hr. Whole-cell lysate was subjected to immunoprecipitation coupled with immunoblotting analysis.

(E and F) 293 cells were transfected with the indicated expression plasmids. Whole-cell lysate was subjected to immunoprecipitation coupled with immunoblotting analysis. IP, immunoprecipitation; IB, immunoblotting. Data are representative of two independent experiments.

was coimmunoprecipitated with IRAK1 and TRAF6, indicating that the N-terminal amphipathic α-helix of Viperin is not necessarily required for its interaction with IRAK1 and TRAF6 (Figures 3E and 3F). These results suggested that Viperin regulates an activation of IRAK1 and TRAF6 to promote TLR7- and TLR9-mediated IFN production in pDC.

Viperin Facilitates the K63-Linked Ubiquitination of IRAK1 to Promote the Production of Type I IFN

TRAF6 is an E3 ubiquitin ligase and mediates the signals from Toll and IL-1 receptors by inducing K63-linked ubiquitination of various regulators including IRAK1 (Liu et al., 2005; Conze et al., 2008; Bhoj and Chen, 2009). Because Viperin interacted

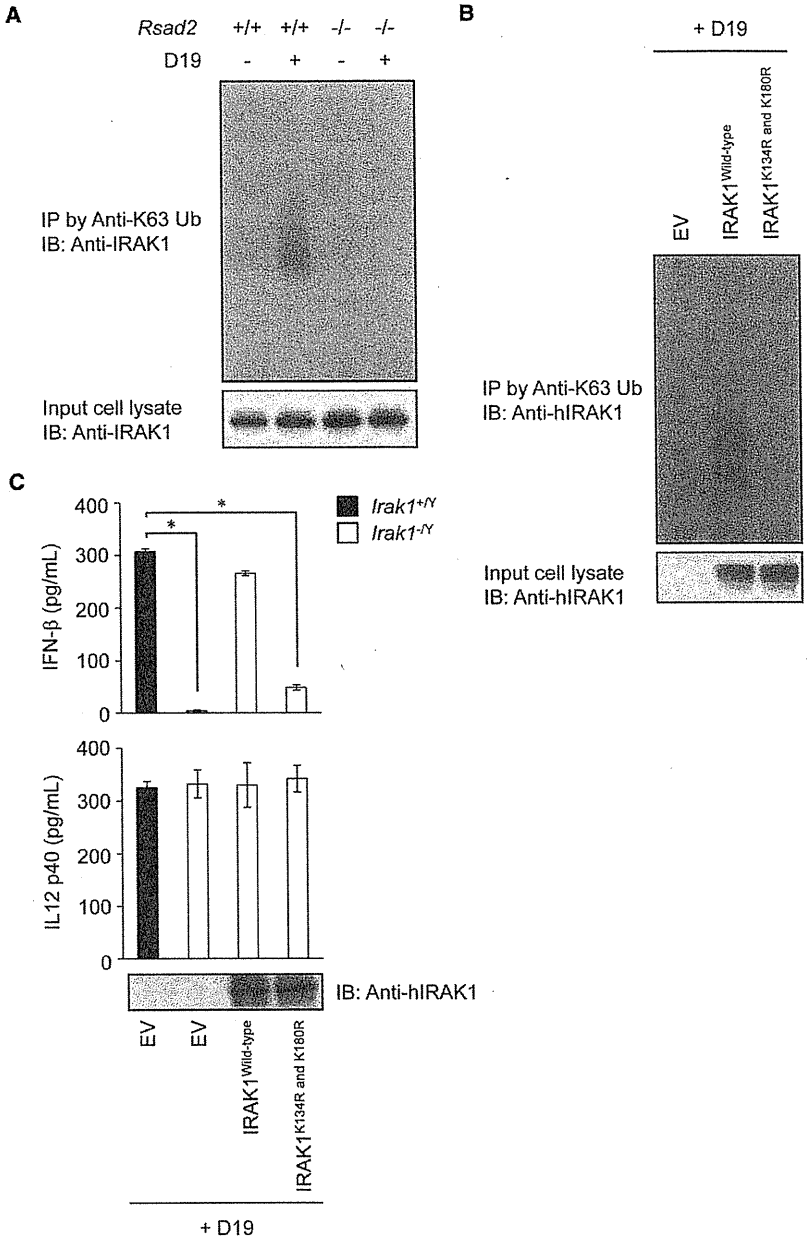

Figure 4. Viperin Facilitates K63-Linked Ubiquitination of IRAK1 in Plasmacytoid Dendritic Cells

(A) *Rsad2*$^{+/+}$ or *Rsad2*$^{-/-}$ FLT3L-induced bone-marrow dendritic cells were stimulated with D19 (1 μM) for 5 hr. Whole-cell lysate was subjected to immunoprecipitation coupled with immunoblotting analysis.

(B) IRAK1$^{wild\text{-}type}$ or IRAK1$^{K134R\ and\ K180R}$ protein was expressed in bone marrow cells isolated from C57/BL6 mice. The transduced cells were cultured in the presence of FLT3L for 7 days and were stimulated with D19 (1 μM) for 5 hr. Whole-cell lysate was subjected to immunoprecipitation coupled with immunoblotting analysis. IP, immunoprecipitation; IB, immunoblotting.

(C) IRAK1$^{wild\text{-}type}$ or IRAK1$^{K134R\ and\ K180R}$ protein was expressed in bone marrow cells isolated from *Irak1*$^{-/Y}$ mice. The transduced cells were cultured in the presence of FLT3L for 7 days and were then stimulated with D19 (1 μM) for 24 hr. Culture supernatant and whole-cell lysate were subjected to ELISA and immunoblotting analysis respectively. EV, Empty vector. The results shown are mean ± SD. Statistical significance (p value) was determined by the Student's t test. *$p < 0.01$. Data are representative of three independent experiments.

with IRAK1 and TRAF6, we assessed the status of K63-linked ubiquitination on IRAK1 in the presence or absence of Viperin. K63-linked ubiquitination of IRAK1, which was induced by A- and D-type CpG DNA, was attenuated in *Rsad2*$^{-/-}$ FLT3L-DCs (Figure 4A). Complementation of wild-type IRAK1, but not the Lys134Arg and Lys180Arg IRAK1 mutant, which is defective in K63-linked ubiquitination by TRAF6 (Figure 4B) (Conze et al., 2008), into *Irak1*$^{-/Y}$ FLT3L-DCs restored the production of IFN-β induced by the engagement of TLR9 (Figure 4C). The K63-linked ubiquitination of IRAK1 induced by the ectopic expression of TRAF6 is not regulated by Viperin, suggesting that Viperin doesn't directly support ubiquitination of IRAK1 by TRAF6. (Figure S4) These results indicated that Viperin promotes TLR7 and TLR9-dependent production of IFN-β production by facilitating K63-linked ubiquitination of IRAK1.

Recruitment of IRAK1 and TRAF6 to Lipid Bodies by Viperin

We investigated the localization of Viperin in pDCs, and found that Viperin localized on the cytoplasmic punctuate structures (Figure 5A). It has been reported that Viperin anchors to the cytosolic face of adipocyte differentiation-related protein (ADRP)-positive lipid-enriched compartments known as lipid droplets and that DCs have ADRP-positive lipid-enriched compartments, termed lipid bodies, to promote the immune response (Hinson and Cresswell, 2009a; Bougnères et al., 2009). On the basis of these reports, we examined whether Viperin localizes on the lipid bodies in DCs. Viperin localized on the punctate structures positive for the ADRP protein (Figure 5A) (Bougnères et al., 2009). The chemical inhibitor U18666A, which disrupts formation of lipid-enriched compartments by reducing up-take of lipids, attenuated TLR7- and TLR9-dependent production of type I IFN by FLT3-induced DCs, indicating the importance of lipid bodies for the signal transduction (Figure 5B). IRAK1 and TRAF6 also localized on the punctate structures in pDC after TLR9 stimulation (Figures 6A and 6B). Both endogenous and exogenously expressed Viperin colocalized with

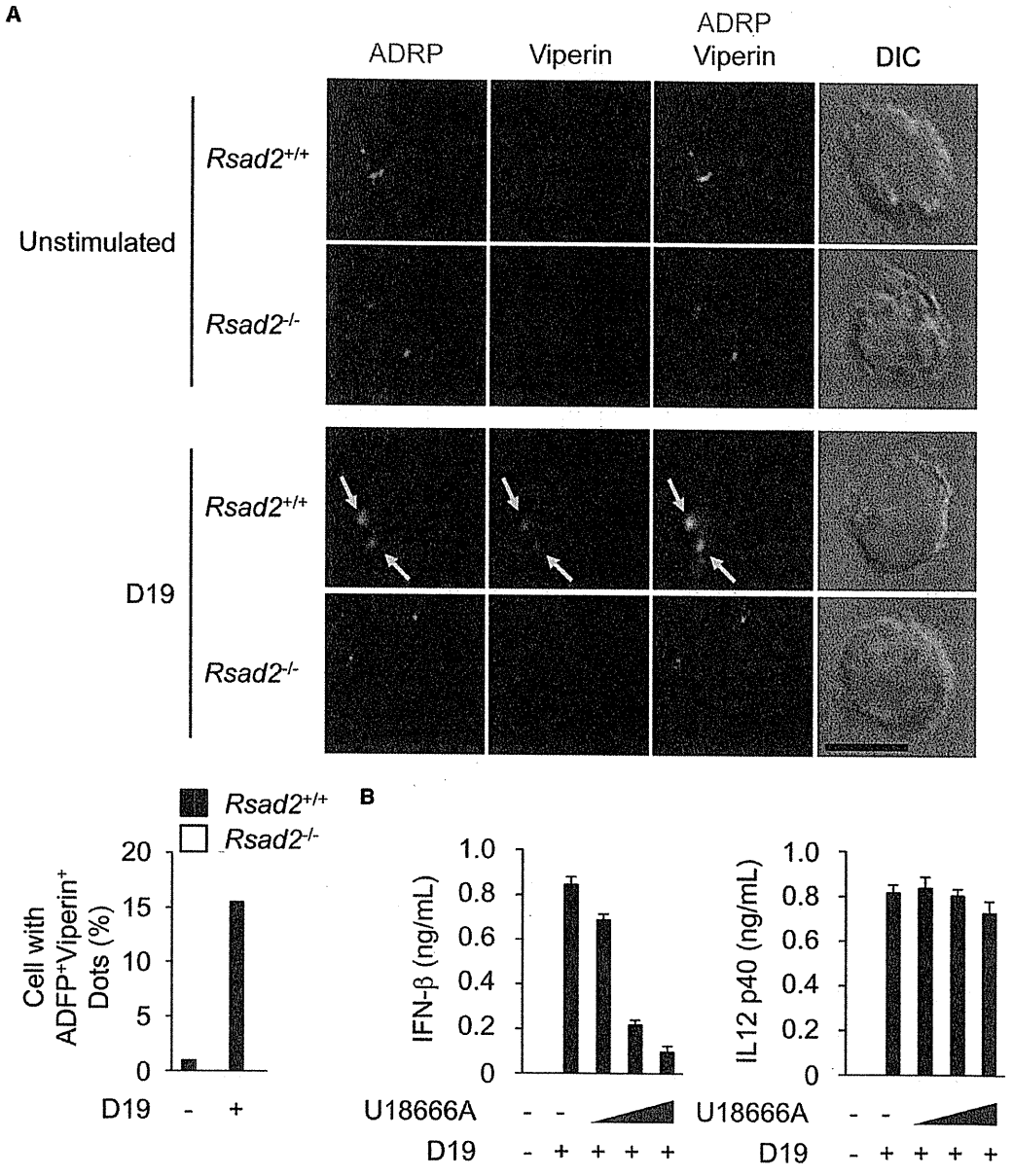

Figure 5. Viperin Localizes on Lipid Bodies in Plasmacytoid Dendritic Cells

(A) *Rsad2*$^{+/+}$ or *Rsad2*$^{-/-}$ FLT3L-induced bone marrow dendritic cells were stimulated with D19 (1 μM) for 5 hr. The cells were fixed with 3% paraformaldehyde and subjected to immunocytochemistry. The B220^{+} dendritic cells were examined under a fluorescent microscope. Yellow arrows indicate the co-localization. DIC, differential interference contrast. The scale bar represents 5 μm. The percentage of B220^{+} dendritic cells with ADRP^{+}Viperin^{+} dots was measured (n = 200 each).

(B) *Rsad2*$^{+/+}$ or *Rsad2*$^{-/-}$ FLT3L-induced bone-marrow dendritic cells were pretreated with U18666A for 16 hr and then stimulated with D19 (1 μM). Culture supernatant collected 24 hr after stimulation was subjected to ELISA. The results shown are mean ± SD.

IRAK1 and TRAF6 on the punctate structures positive for the BODIPY dye, a marker of lipid bodies, in pDC after TLR9 stimulation (Figures 6A and 6B and Figures S5A–S5D). Viperin deficiency disrupted the localization of IRAK1 and TRAF6 on the BODIPY-positive punctate structures (Figures 6A and 6B).

Although TLR9 localized on the Viperin-positive lipid bodies with low frequency, MyD88 localized on Viperin-positive lipid bodies with moderate frequency (Figures S5E and S5F), suggesting that MyD88 mediates the signals from TLR9 on the lysosomes to IRAK1 and TRAF6 on the lipid bodies. Viperin also colocalized with IRF7 in response to CpG DNA and facilitated the subsequent nuclear translocation of IRF7, which is mediated by IRAK1 (Figure 7). Viperin might form a large complex with IRF7 and IRAK1 because IRF7 was coimmunoprecipitated with IRAK1 and Viperin when these factors were ectopically expressed in 293 cells (Figure S6). These results indicated that Viperin is

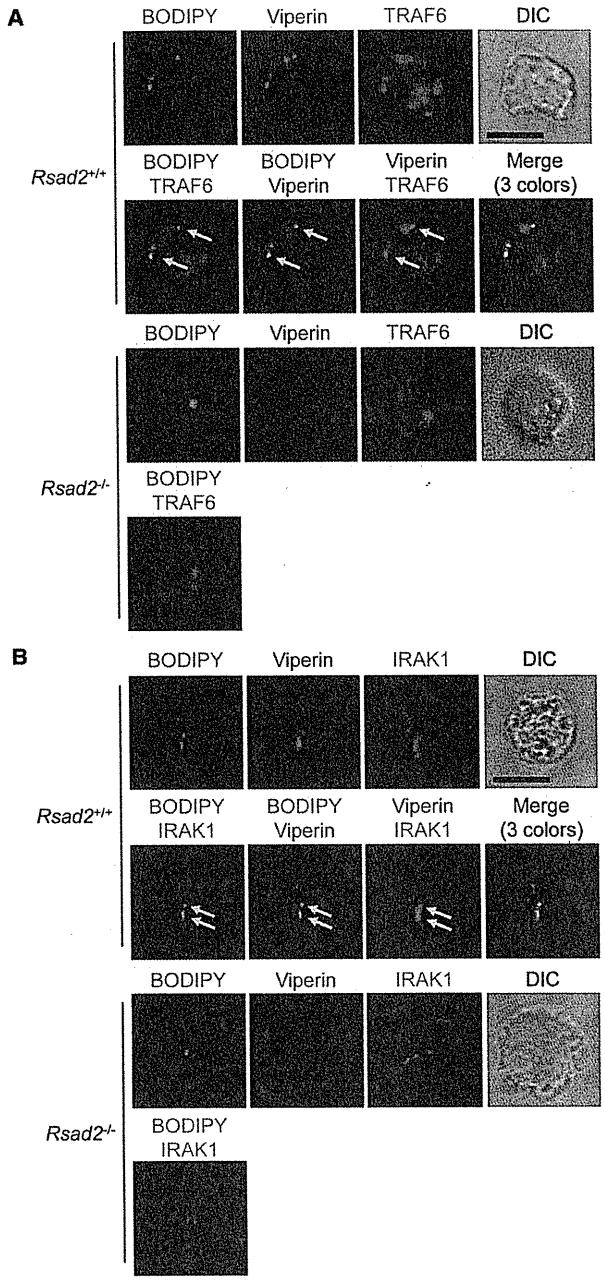

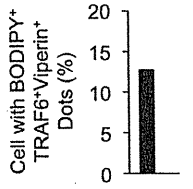

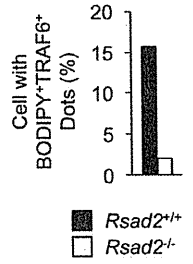

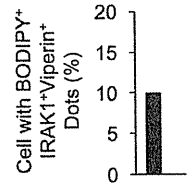

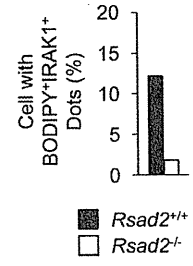

Figure 6. Viperin Recruits IRAK1 and TRAF6 to the Lipid Bodies

(A and B) *Rsad2*$^{+/+}$ or *Rsad2*$^{-/-}$ FLT3L-induced bone-marrow dendritic cells were stimulated with D19 (1 μM) for 5 hr. The cells were fixed with 3% paraformaldehyde and subjected to immunocytochemistry. The B220^{+} dendritic cells were examined under a fluorescent microscope. Yellow arrows indicate the colocalization. DIC, differential interference contrast. The scale bar represents 5 μm. The percentage of B220^{+} dendritic cells with the indicated dots was measured (n = 400 each).

important for the recruitment of IRAK1 and TRAF6 to the lipid bodies, which are the transfer points in the TLR7 and TLR9 signaling pathway leading to the activation of IRF7.

DISCUSSION

It has become clear that intracellular membrane-surrounded compartments play pivotal roles in the signal transduction from PRRs detecting viral nucleic acids (Saitoh and Akira, 2010). The signals from RLR are mediated by an adaptor protein, IPS-1 (also known as MAVS, VISA, or CARDIF), which is expressed on mitochondria and peroxisomes (Seth et al., 2005; Dixit et al., 2010). Furthermore the dsDNA-induced innate immune response requires the dynamic translocation of STING, a multispanning membrane protein, from ER to cytoplasmic membrane-bound structures (Ishikawa et al., 2009; Saitoh et al., 2009). In the present study, we demonstrated that the N-terminal amphipathic α-helix of Viperin is required for its function, indicating that Viperin anchors on the membrane lipid layer of lipid bodies and mediates the signal from TLR7 and TLR9. Viperin recruits IRAK1 and TRAF6 to the lipid bodies in a stimulation-dependent manner and facilitates the subsequent K63-linked ubiquitination of IRAK1 by TRAF6, which results in the IRF7-mediated induction of type I IFN. Thus, the lipid bodies are the major transit points in the TLR7 and TLR9 signaling pathway leading to the production of type I IFN in pDCs.

Although IRAK1 is specifically involved in TLR-IL-1R signaling pathway, TRAF6 is critical in the signal transduction from various immune-related receptors, such as T cell receptor (TCR), RANK, CD40, and TLR-IL-1R. Because it has been reported that Viperin mediates TCR-induced activation of NF-κB and AP-1, it would be of interest to assess whether Viperin promotes Bcl10-dependent K63-linked ubiquitination of NEMO by TRAF6, an essential process of NF-κB activation induced by TCR (Liu et al., 2005; Qiu et al., 2009; Bhoj and Chen, 2009).

A mechanism underlying the translocation of Viperin from the ER to lipid bodies is still not known, whereas Unc93B1-dependent translocation of TLR7 and TLR9 from the ER to endolysosomes has been revealed (Latz et al., 2004; Kim et al., 2008). In this context, it would be of interest to assess the involvement of autophagy-related proteins, regulators of membrane trafficking (Saitoh and Akira, 2010), for the localization of Viperin

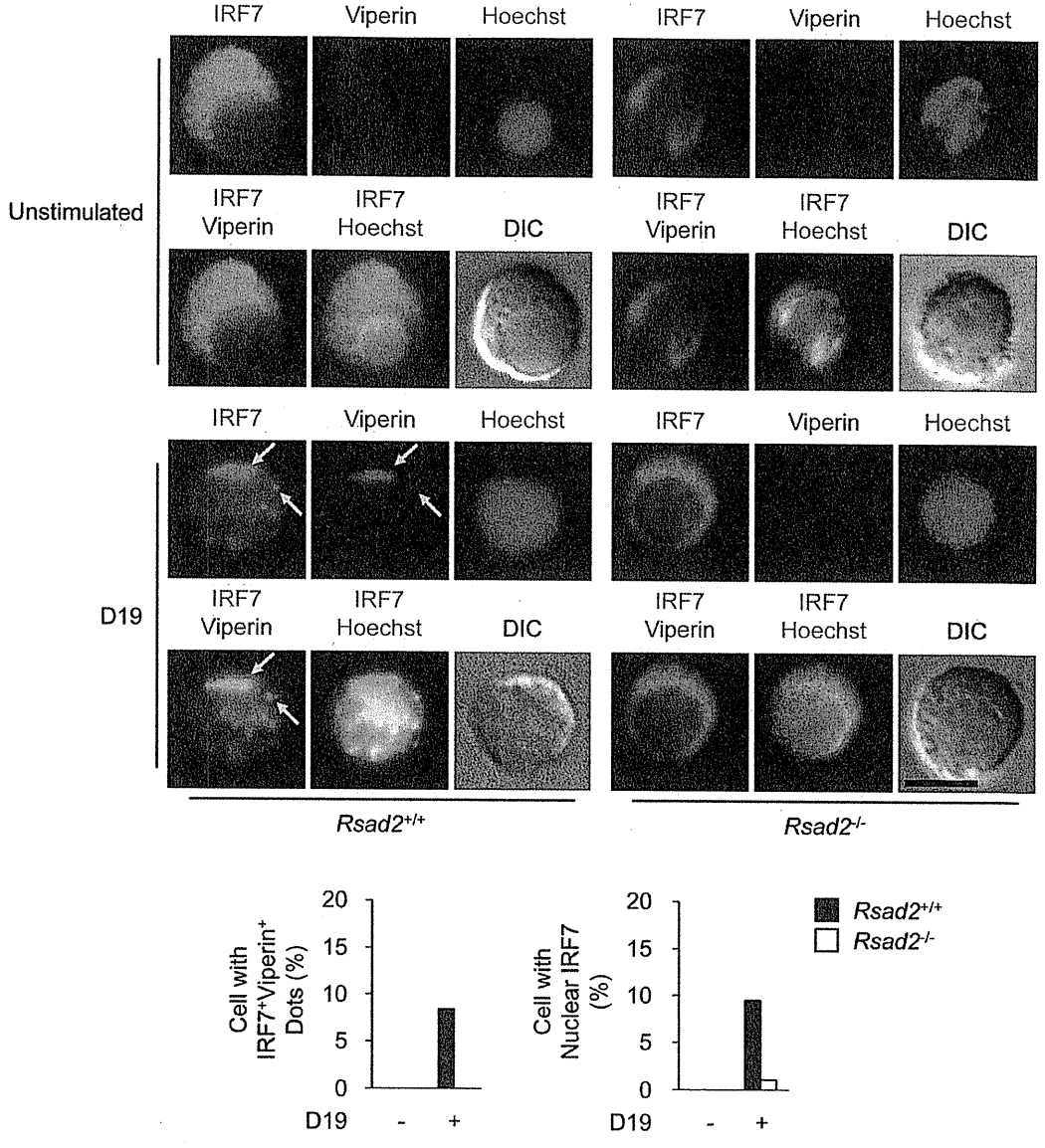

Figure 7. Viperin Colocalizes with IRF7 and Promotes the Nuclear Translocation of IRF7 after TLR9 Stimulation
Flag-tagged IRF7 protein was expressed in bone-marrow cells isolated from *Rsad2*$^{+/+}$ or *Rsad2*$^{-/-}$ mice. The transduced cells were cultured in the presence of FLT3L for 7 days and stimulated with D19 (1 μM) for 5 hr. The cells were fixed with 3% paraformaldehyde and were subjected to immunocytochemistry. The B220^{+} dendritic cells were examined under a fluorescent microscope. Yellow arrows indicate the colocalization. DIC, differential interference contrast. The scale bar represents 5 μm. The percentage of B220^{+} dendritic cells with IRF7^{+}Viperin^{+} dots or with nuclear IRF7 was measured (n = 200 each).

on the lipid bodies. This is because Atg5, an autophagy-related protein, is involved in the production of type I IFN by A- and D-type CpG DNA as well as in the recognition of the viral genome by TLR7 and TLR9 (Lee et al., 2007). Atg7, another autophagy-related protein, regulates the number and the size of lipid-enriched compartments in various types of cells (Czaja, 2010). Furthermore, autophagy-related proteins are involved in the translocation of membrane associated IFN-γ-inducible p47 GTPase IIGP1 from the ER or Golgi apparatus to the lamp1-positive compartments after infection by *Toxoplasma gondii* (Zhao et al., 2008). Further studies will be required to address this issue.

Viperin has been considered a radical SAM enzyme, given that it harbors a CX_3CX_2C motif as well as some additional motifs conserved in the radical SAM enzyme family (Duschene and Broderick, 2010; Shaveta et al., 2010). It has been shown that SAM is the methyl donor in the biological reaction and the precursor of polyamines, which are often involved in the regulation of cellular responses (Duschene and Broderick, 2010; Shaveta et al., 2010). Radical SAM enzymes induce cleavage

of SAM to generate the 5′-deoxyadenosyl radical, which contributes to the cleavage of C-H bonds in the alkyl group and alters the local concentration of SAM (Duschene and Broderick, 2010; Shaveta et al., 2010). Recent studies have uncovered that purified Viperin protein could contain a $[4Fe\text{-}4S]^{+}$ cluster under anaerobic conditions and induce the cleavage of SAM in vitro, suggesting that Viperin acts as a radical SAM enzyme during the antiviral response (Duschene and Broderick, 2010; Shaveta et al., 2010). Indeed, mutations in the CX_3CX_2C motif of the Viperin protein disrupt its ability to suppress the replication of certain types of RNA viruses (Jiang et al., 2008; Jiang et al., 2010). However, the exact mechanism through which the radical SAM enzyme alters the function of Viperin on viral replication remains unknown. We have observed partial involvement of the CX_3CX_2C motif in the Viperin protein with regulation of the TLR7 and TLR9-mediated production of type I IFN; it is difficult to clarify the exact function of the Viperin CX_3CX_2C motif. In future studies, identification of the chemical reaction catalyzed by the radical SAM enzyme domain of Viperin would be important in revealing the molecular function of Viperin during the antiviral response.

Type I IFN triggers orchestrated expression of antiviral proteins. Each IFN-inducible protein contributes to the antiviral response at various stages and protects the host suffering from viral infection. We here provide evidence that Viperin, the IFN-inducible protein, acts as a regulator for PRR-mediated innate immune response. Thus, Viperin plays dual roles: a direct suppression of viral replication as reported and a facilitation of TLR7- and TLR9-mediated production of type I IFN. Our study provides insight into the role of Viperin in the regulation of host defense responses to viruses. Although various IFN-inducible proteins, such as the APOBEC family and Zinc finger antiviral proteins, contribute to the direct suppression of viral replication, it remains unclear whether such molecules are involved in the regulation of PRR-triggered signaling pathways (Wolf and Goff, 2008; Neil and Bieniasz, 2009). Therefore revalidation of the roles of IFN-inducible proteins in PRR-mediated innate immune responses will be needed for better understanding of host defense.

EXPERIMENTAL PROCEDURES

Mice and Cells

The methods for the generation of Viperin-deficient mice are described in the Supplemental Experimental Procedures. *Irak1*$^{-/Y}$ mice were kindly donated by J.A. Thomas (University of Texas Southwestern Medical Center, Texas, USA). *Irf3*$^{-/-}$ and *Irf7*$^{-/-}$ mice were kindly donated by T. Taniguchi (University of Tokyo, Tokyo, Japan). Mouse splenic plasmacytoid dendritic cells were isolated with a Plasmacytoid Dendritic Cell Isolation Kit II (Miltenyi Biotec). Mouse bone marrow dendritic cells and mouse thioglycollate-elicited peritoneal macrophages were prepared as previously described (Kato et al., 2006; Saitoh et al., 2008).

Mice were maintained in our animal facility and treated in accordance with the guidelines of Osaka University.

Viruses and Bacteria

NDV has been described previously (Kato et al., 2006). *Salmonella typhimurium* (SR-11 × 3181) was provided by the Kitasato Institute for Life Science. *Listeria monocytogenes* was described previously (Uematsu et al., 2007).

Reagents

ADRP antibody was purchased from Abcam. Anti-IRAK1 and anti-Myc antibodies were purchased from Cell Signaling Technology. Actin and TRAF6 antibodies were purchased from Santa Cruz Biotechnology. Viperin antibody was purchased from Hycult biotech. Ubiquitin (Lys63-specific clone Apu3) antibody was purchased from Millipore. Flag antibody and Poly (dA-dT) were purchased from Sigma. Poly (rI-rC) was purchased from GE Healthcare. Depleted zymosan, FITC-labeled ODN1585, Flagellin, LPS, and Pam3CSK4 were purchased from Invivogen. R848 was purchased from Alexis. Curdlan was purchased from WAKO. Lipofectamine 2000, BODIPY, and alexa-labeled secondary antibodies were purchased from Invitrogen. ELISA kits for mouse CXCL10 and IL-12 p40 were purchased from R&D Systems. ELISA kits for mouse IFN-α and IFN-β, and recombinant mouse IFN-β were purchased from PBL InterferonSource. Recombinant mouse GMCSF and human FLT3L were purchased from Peprotech. D19, D35, and ODN1668 were synthesized as described previously (Kawagoe et al., 2007).

Plasmids

pcDNA3.1 (+) was purchased from Invitrogen. The retroviral expression construct pMX was kindly donated by T. Kitamura (The University of Tokyo, Tokyo, Japan). pMRX, a derivative of pMX, was kindly donated by S. Yamaoka (Tokyo Medical and Dental University, Tokyo, Japan). pMRX-ires-puro and pMRX-ires-bsr have been described previously (Saitoh et al., 2003). Complementary DNA encoding the Myc-tag sequence and mouse Viperin was inserted into pcDNA3.1 (+) and pMRX-ires-puro, generating pcDNA3-Myc-Viperin and pMRX-Myc-Viperin-ires-puro, respectively. Complementary DNA encoding the Flag-tag sequence and mouse IRF7 was inserted into pMRX-ires-puro, generating pMRX-IRF7-Flag-ires-puro. Complementary DNA encoding IRAK1$^{\text{wild-type}}$ or IRAK1$^{\text{K134R and K180R}}$ was amplified by PCR with pcDNA3-V5-IRAK1$^{\text{Wild-type}}$ or pcDNA3-V5-IRAK1$^{\text{K134R and K180R}}$ (kind gifts from J.D. Ashwell; National Cancer Institute, Maryland, USA) as a template. The inserts were cloned into pMRX-ires-puro, generating pMRX-IRAK1$^{\text{WT}}$-ires-puro and pMRX-IRAK1$^{\text{K134R and K180R}}$-ires-puro, respectively. The expression plasmids for Flag-tagged MyD88, IRAK4, IRAK1, TRAF6, and IRF7 have been described previously (Kawai et al., 2004; Uematsu et al., 2005). The pCMV-3xFlag hTRAF3 plasmid was provided by T. Yasui (Osaka University, Osaka, Japan).

Retroviral Gene Transduction

The Plat-E cells used for the generation of recombinant retrovirus were kindly donated by T. Kitamura (The University of Tokyo, Tokyo, Japan). Retroviral infection was performed as previously described (Saitoh et al., 2008).

RT-PCR

Total RNA was isolated with RNAeasy Mini kits (QIAGEN) in accordance with the manufacturer's instructions. Reverse transcription was performed with ReverTra Ace (TOYOBO) in accordance with the manufacturer's instructions.

For quantitative PCR, cDNA fragments were amplified by Real-Time PCR Master Mix (TOYOBO) in accordance with the manufacturer's instructions. Fluorescence from the TaqMan probe for each cytokine was detected by a 7500 Real-Time PCR System (Applied Biosystems). For determining the relative induction of IFN-β and IL12 p40 mRNA, the mRNA expression level of each gene was normalized to the expression level of 18S RNA.

Immunoblotting and Immunoprecipitation

Immunoblotting and immunoprecipitation were performed as previously described (Saitoh et al., 2006).

ELISA

The level of cytokine production was measured by ELISA in accordance with the manufacturer's instructions.

Immunocytochemistry

Immunofluorescence staining was performed as previously described (Saitoh et al., 2008). In brief, the paraformaldehyde fixed cells were permeabilized with saponin and were incubated in PBS with 1% goat serum and 5% fetal calf serum (FCS) for the blocking. The immunofluorescence staining was performed in FCS-containing PBS with the indicated antibodies and then with the appropriate fluorescent dye-labeled secondary antibodies. The cells were subsequently stained with biotin-labeled anti-B220 antibody and

Streptavidin-Qdot625. Samples were examined under an IX81-DSU spinning disc confocal microscope (Olympus).

Intracellular IFN-α Staining

Flt3L-induced bone marrow DCs were stimulated with D19 (1 μM) for 5 hr and were cultured in the presence of Golgi stop for an additional 3 hr. The cells were fixed in paraformaldehyde and permeabilized by saponin-containing buffer. The cells was stained by a mixture of rat anti-mouse IFN-α antibodies (clone F18 purchased from Hycult Biotechnology and clone RMMA-1 purchased from PBL Biomedical Laboratories) and subsequently by biotinylated mouse anti-rat IgG antibody (Jackson Immuno Research Laboratories) and Streptavidin-APC. The cells were subsequently stained with PE-labeled anti-B220 antibody and analyzed on a FACS Calibur (BD Biosciences).

SUPPLEMENTAL INFORMATION

Supplemental Information includes Supplemental Experimental Procedures and six figures and can be found with this article online at doi:10.1016/j.immuni.2011.03.010.

ACKNOWLEDGMENTS

We are grateful to J.A. Thomas, J.D. Ashwell, S. Yamaoka, T. Kitamura, T. Yasui, and Y. Kawaguchi for providing invaluable materials. We thank the members of the Laboratory of Host Defense for discussion; K. Yamamoto, M. Kumagai, N. Ishizawa, and Y. Fujiwara for technical assistance; and E. Kamada for secretarial assistance. This work was in part supported by grants from the Ministry of Education, Culture, Sports, Science, and Technology in Japan, from the Ministry of Health, Labour and Welfare in Japan, and from the 21st Century Center of Excellence Program of Japan, and from NIH (AI070167) to S.A. This research was also supported by the Japan Society for the Promotion of Science through its "Funding Program for World-Leading Innovative R&D on Science and Technology (FIRST Program)" to S.A. T. S. generated Viperin-deficient mice and performed the immunological research. N.Y. contributed the expression vectors. O.T, S.U., T. K., and T.S. contributed the immunological research. S.A. designed overall research and wrote the paper.

Received: September 3, 2010
Revised: December 7, 2010
Accepted: December 29, 2010
Published online: March 24, 2011

REFERENCES

Bhoj, V.G., and Chen, Z.J. (2009). Ubiquitylation in innate and adaptive immunity. Nature *458*, 430–437.

Blasius, A.L., and Beutler, B. (2010). Intracellular toll-like receptors. Immunity *32*, 305–315.

Bougnères, L., Helft, J., Tiwari, S., Vargas, P., Chang, B.H., Chan, L., Campisi, L., Lauvau, G., Hugues, S., Kumar, P., et al. (2009). A role for lipid bodies in the cross-presentation of phagocytosed antigens by MHC class I in dendritic cells. Immunity *31*, 232–244.

Chin, K.C., and Cresswell, P. (2001). Viperin (cig5), an IFN-inducible antiviral protein directly induced by human cytomegalovirus. Proc. Natl. Acad. Sci. USA *98*, 15125–15130.

Conze, D.B., Wu, C.J., Thomas, J.A., Landstrom, A., and Ashwell, J.D. (2008). Lys63-linked polyubiquitination of IRAK-1 is required for interleukin-1 receptor- and toll-like receptor-mediated NF-kappaB activation. Mol. Cell. Biol. *28*, 3538–3547.

Czaja, M.J. (2010). Autophagy in health and disease. 2. Regulation of lipid metabolism and storage by autophagy: Pathophysiological implications. Am. J. Physiol. Cell Physiol. *298*, C973–C978.

Dixit, E., Boulant, S., Zhang, Y., Lee, A.S., Odendall, C., Shum, B., Hacohen, N., Chen, Z.J., Whelan, S.P., Fransen, M., et al. (2010). Peroxisomes are signaling platforms for antiviral innate immunity. Cell *141*, 668–681.

Duschene, K.S., and Broderick, J.B. (2010). The antiviral protein viperin is a radical SAM enzyme. FEBS Lett. *584*, 1263–1267.

Gotoh, K., Tanaka, Y., Nishikimi, A., Nakamura, R., Yamada, H., Maeda, N., Ishikawa, T., Hoshino, K., Uruno, T., Cao, Q., et al. (2010). Selective control of type I IFN induction by the Rac activator DOCK2 during TLR-mediated plasmacytoid dendritic cell activation. J. Exp. Med. *207*, 721–730.

Häcker, H., Redecke, V., Blagoev, B., Kratchmarova, I., Hsu, L.C., Wang, G.G., Kamps, M.P., Raz, E., Wagner, H., Häcker, G., et al. (2006). Specificity in Toll-like receptor signalling through distinct effector functions of TRAF3 and TRAF6. Nature *439*, 204–207.

Hinson, E.R., and Cresswell, P. (2009a). The antiviral protein, viperin, localizes to lipid droplets via its N-terminal amphipathic alpha-helix. Proc. Natl. Acad. Sci. USA *106*, 20452–20457.

Hinson, E.R., and Cresswell, P. (2009b). The N-terminal amphipathic alpha-helix of viperin mediates localization to the cytosolic face of the endoplasmic reticulum and inhibits protein secretion. J. Biol. Chem. *284*, 4705–4712.

Honda, K., Yanai, H., Mizutani, T., Negishi, H., Shimada, N., Suzuki, N., Ohba, Y., Takaoka, A., Yeh, W.C., and Taniguchi, T. (2004). Role of a transductional-transcriptional processor complex involving MyD88 and IRF-7 in Toll-like receptor signaling. Proc. Natl. Acad. Sci. USA *101*, 15416–15421.

Honda, K., Takaoka, A., and Taniguchi, T. (2006). Type I interferon [corrected] gene induction by the interferon regulatory factor family of transcription factors. Immunity *25*, 349–360.

Hoshino, K., Sugiyama, T., Matsumoto, M., Tanaka, T., Saito, M., Hemmi, H., Ohara, O., Akira, S., and Kaisho, T. (2006). IkappaB kinase-alpha is critical for interferon-alpha production induced by Toll-like receptors 7 and 9. Nature *440*, 949–953.

Hoshino, K., Sasaki, I., Sugiyama, T., Yano, T., Yamazaki, C., Yasui, T., Kikutani, H., and Kaisho, T. (2010). Critical role of IkappaB Kinase alpha in TLR7/9-induced type I IFN production by conventional dendritic cells. J. Immunol. *184*, 3341–3345.

Ichinohe, T., Pang, I.K., and Iwasaki, A. (2010). Influenza virus activates inflammasomes via its intracellular M2 ion channel. Nat. Immunol. *11*, 404–410.

Ishikawa, H., Ma, Z., and Barber, G.N. (2009). STING regulates intracellular DNA-mediated, type I interferon-dependent innate immunity. Nature *461*, 788–792.

Jiang, D., Guo, H., Xu, C., Chang, J., Gu, B., Wang, L., Block, T.M., and Guo, J.T. (2008). Identification of three interferon-inducible cellular enzymes that inhibit the replication of hepatitis C virus. J. Virol. *82*, 1665–1678.

Jiang, D., Weidner, J.M., Qing, M., Pan, X.B., Guo, H., Xu, C., Zhang, X., Birk, A., Chang, J., Shi, P.Y., et al. (2010). Identification of five interferon-induced cellular proteins that inhibit west nile virus and dengue virus infections. J. Virol. *84*, 8332–8341.

Kato, H., Takeuchi, O., Sato, S., Yoneyama, M., Yamamoto, M., Matsui, K., Uematsu, S., Jung, A., Kawai, T., Ishii, K.J., et al. (2006). Differential roles of MDA5 and RIG-I helicases in the recognition of RNA viruses. Nature *441*, 101–105.

Kawagoe, T., Sato, S., Jung, A., Yamamoto, M., Matsui, K., Kato, H., Uematsu, S., Takeuchi, O., and Akira, S. (2007). Essential role of IRAK-4 protein and its kinase activity in Toll-like receptor-mediated immune responses but not in TCR signaling. J. Exp. Med. *204*, 1013–1024.

Kawai, T., and Akira, S. (2010). The role of pattern-recognition receptors in innate immunity: Update on Toll-like receptors. Nat. Immunol. *11*, 373–384.

Kawai, T., Sato, S., Ishii, K.J., Coban, C., Hemmi, H., Yamamoto, M., Terai, K., Matsuda, M., Inoue, J., Uematsu, S., et al. (2004). Interferon-alpha induction through Toll-like receptors involves a direct interaction of IRF7 with MyD88 and TRAF6. Nat. Immunol. *5*, 1061–1068.

Kim, Y.M., Brinkmann, M.M., Paquet, M.E., and Ploegh, H.L. (2008). UNC93B1 delivers nucleotide-sensing toll-like receptors to endolysosomes. Nature *452*, 234–238.

Latz, E., Schoenemeyer, A., Visintin, A., Fitzgerald, K.A., Monks, B.G., Knetter, C.F., Lien, E., Nilsen, N.J., Espevik, T., and Golenbock, D.T. (2004). TLR9 signals after translocating from the ER to CpG DNA in the lysosome. Nat. Immunol. *5*, 190–198.

Lee, H.K., Lund, J.M., Ramanathan, B., Mizushima, N., and Iwasaki, A. (2007). Autophagy-dependent viral recognition by plasmacytoid dendritic cells. Science *315*, 1398–1401.

Liu, Y.C., Penninger, J., and Karin, M. (2005). Immunity by ubiquitylation: A reversible process of modification. Nat. Rev. Immunol. *5*, 941–952.

Medzhitov, R. (2009). Approaching the asymptote: 20 years later. Immunity *30*, 766–775.

Neil, S., and Bieniasz, P. (2009). Human immunodeficiency virus, restriction factors, and interferon. J. Interferon Cytokine Res. *29*, 569–580.

O'Neill, L.A., and Bowie, A.G. (2010). Sensing and signaling in antiviral innate immunity. Curr. Biol. *20*, R328–R333.

Qiu, L.Q., Cresswell, P., and Chin, K.C. (2009). Viperin is required for optimal Th2 responses and T-cell receptor-mediated activation of NF-kappaB and AP-1. Blood *113*, 3520–3529.

Saitoh, T., and Akira, S. (2010). Regulation of innate immune responses by autophagy-related proteins. J. Cell Biol. *189*, 925–935.

Saitoh, T., Nakayama, M., Nakano, H., Yagita, H., Yamamoto, N., and Yamaoka, S. (2003). TWEAK induces NF-kappaB2 p100 processing and long lasting NF-kappaB activation. J. Biol. Chem. *278*, 36005–36012.

Saitoh, T., Tun-Kyi, A., Ryo, A., Yamamoto, M., Finn, G., Fujita, T., Akira, S., Yamamoto, N., Lu, K.P., and Yamaoka, S. (2006). Negative regulation of interferon-regulatory factor 3-dependent innate antiviral response by the prolyl isomerase Pin1. Nat. Immunol. *7*, 598–605.

Saitoh, T., Fujita, N., Jang, M.H., Uematsu, S., Yang, B.G., Satoh, T., Omori, H., Noda, T., Yamamoto, N., Komatsu, M., et al. (2008). Loss of the autophagy protein Atg16L1 enhances endotoxin-induced IL-1beta production. Nature *456*, 264–268.

Saitoh, T., Fujita, N., Hayashi, T., Takahara, K., Satoh, T., Lee, H., Matsunaga, K., Kageyama, S., Omori, H., Noda, T., et al. (2009). Atg9a controls dsDNA-driven dynamic translocation of STING and the innate immune response. Proc. Natl. Acad. Sci. USA *106*, 20842–20846.

Schroder, K., and Tschopp, J. (2010). The inflammasomes. Cell *140*, 821–832.

Seth, R.B., Sun, L., Ea, C.K., and Chen, Z.J. (2005). Identification and characterization of MAVS, a mitochondrial antiviral signaling protein that activates NF-kappaB and IRF 3. Cell *122*, 669–682.

Severa, M., Coccia, E.M., and Fitzgerald, K.A. (2006). Toll-like receptor-dependent and -independent viperin gene expression and counter-regulation by PRDI-binding factor-1/BLIMP1. J. Biol. Chem. *281*, 26188–26195.

Shaveta, G., Shi, J., Chow, V.T., and Song, J. (2010). Structural characterization reveals that viperin is a radical S-adenosyl-L-methionine (SAM) enzyme. Biochem. Biophys. Res. Commun. *391*, 1390–1395.

Takeuchi, O., and Akira, S. (2010). Pattern recognition receptors and inflammation. Cell *140*, 805–820.

Uematsu, S., Sato, S., Yamamoto, M., Hirotani, T., Kato, H., Takeshita, F., Matsuda, M., Coban, C., Ishii, K.J., Kawai, T., et al. (2005). Interleukin-1 receptor-associated kinase-1 plays an essential role for Toll-like receptor (TLR)7- and TLR9-mediated interferon-alpha induction. J. Exp. Med. *201*, 915–923.

Uematsu, S., Kaisho, T., Tanaka, T., Matsumoto, M., Yamakami, M., Omori, H., Yamamoto, M., Yoshimori, T., and Akira, S. (2007). The C/EBP beta isoform 34-kDa LAP is responsible for NF-IL-6-mediated gene induction in activated macrophages, but is not essential for intracellular bacteria killing. J. Immunol. *179*, 5378–5386.

Wang, X., Hinson, E.R., and Cresswell, P. (2007). The interferon-inducible protein viperin inhibits influenza virus release by perturbing lipid rafts. Cell Host Microbe *2*, 96–105.

Wolf, D., and Goff, S.P. (2008). Host restriction factors blocking retroviral replication. Annu. Rev. Genet. *42*, 143–163.

Yoneyama, M., and Fujita, T. (2010). Recognition of viral nucleic acids in innate immunity. Rev. Med. Virol. *20*, 4–22.

Zhao, Z., Fux, B., Goodwin, M., Dunay, I.R., Strong, D., Miller, B.C., Cadwell, K., Delgado, M.A., Ponpuak, M., Green, K.G., et al. (2008). Autophagosome-independent essential function for the autophagy protein Atg5 in cellular immunity to intracellular pathogens. Cell Host Microbe *4*, 458–469.

IL-1α Modulates Neutrophil Recruitment in Chronic Inflammation Induced by Hydrocarbon Oil

Pui Y. Lee,*,†,[1] Yutaro Kumagai,*,‡,[1] Yuan Xu,*,† Yi Li,*,† Tolga Barker,*,† Chao Liu,*,† Eric S. Sobel,*,† Osamu Takeuchi,‡ Shizuo Akira,‡ Minoru Satoh,*,†,§ and Westley H. Reeves*,†,§

Exposure to naturally occurring hydrocarbon oils is associated with the development of chronic inflammation and a wide spectrum of pathological findings in humans and animal models. The mechanism underlying the unremitting inflammatory response to hydrocarbons remains largely unclear. The medium-length alkane 2,6,10,14 tetramethylpentadecane (also known as pristane) is a hydrocarbon that potently elicits chronic peritonitis characterized by persistent infiltration of neutrophils and monocytes. In this study, we reveal the essential role of IL-1α in sustaining the chronic recruitment of neutrophils following 2,6,10,14 tetramethylpentadecane treatment. IL-1α and IL-1R signaling promote the migration of neutrophils to the peritoneal cavity in a CXCR2-dependent manner. This mechanism is at least partially dependent on the production of the neutrophil chemoattractant CXCL5. Moreover, although chronic infiltration of inflammatory monocytes is dependent on a different pathway requiring TLR-7, type I IFN receptor, and CCR2, the adaptor molecules MyD88, IL-1R–associated kinase (IRAK)-4, IRAK-1, and IRAK-2 are shared in regulating the recruitment of both monocytes and neutrophils. Taken together, our findings uncover an IL-1α–dependent mechanism of neutrophil recruitment in hydrocarbon-induced peritonitis and illustrate the interactions of innate immune pathways in chronic inflammation. *The Journal of Immunology*, **2011, 186: 1747–1754.**

Chronic inflammation is characterized by unremitting immune responses to persistent microbial infection or chemical agents (1). Continued influx of leukocytes and local production of inflammatory mediators are common features at sites of chronic inflammation. Although chemokine gradients play a prominent role in leukocyte migration, the mechanisms responsible for the sustained chemokine production and subsequent influx of neutrophils and monocytes in chronic inflammation are not well defined.

Exposure to naturally occurring hydrocarbon oils is associated with the development of chronic inflammation and a variety of pathological findings in humans and animal models (2–5). Due to their ability to enhance and sustain inflammation, hydrocarbons are often used as adjuvants in vaccines (6, 7). Among the most potent hydrocarbons in eliciting chronic inflammation is the medium-length alkane 2,6,10,14 tetramethylpentadecane (TMPD; also known as pristane). A single i.p. dose of TMPD elicits infiltration of neutrophils and monocytes into the peritoneal cavity for several months (8). The chronic inflammatory response promotes the formation of plasmacytomas and lipogranulomas, a form of ectopic lymphoid tissue (5, 9). Depending on the genetic background, persistent inflammation in TMPD-treated mice also promotes the development of a plethora of autoimmune manifestations including autoantibodies, glomerulonephritis, arthritis, and pulmonary vasculitis (9–13). In addition, TMPD augments mAb production by hybridoma cells by stimulating IL-6 production (14).

Recent studies have begun to unravel the mechanisms responsible for the chronic inflammation induced by TMPD. The response to TMPD is orchestrated by major components of the innate immune system. The continued influx of Ly6C^{hi} inflammatory monocytes to the peritoneal cavity requires the presence of type I IFN (IFN-I) production downstream of TLR-7 signaling (15). IFN-I activates the production of the monocyte chemoattractants CCL2, CCL7, and CCL12, which collectively recruit monocytes to the site of inflammation in a CCR2-dependent manner (16). The persistent infiltration of neutrophils, in contrast, remains largely unexplained. In this study, we aimed to define the mechanism of neutrophil recruitment in TMPD-induced chronic inflammation.

Materials and Methods

Mice

These studies were approved by the Institutional Animal Care and Use Committee. Wild-type C57BL/6, TNF-α$^{-/-}$, CCR2$^{-/-}$, and IL-1R$^{-/-}$ mice (all on a C57BL/6 background), BALB/c, CXCR2$^{-/-}$ (BALB/c background), C3H/HeJ, C3H/HeOuJ, and CBA/CaJ mice were from The Jackson Laboratory (Bar Harbor, ME). FcRγ-chain$^{-/-}$ mice were from Taconic Farms (Hudson, NY), and 129/Sv mice were from B&K Universal Limited (Grimston, Aldbrough, England). Mice were maintained in a specific pathogen-free facility at the Malcolm Randall Veterans Affairs Medical Center (Gainesville, FL). MyD88$^{-/-}$, apoptosis-associated speck-

*Division of Rheumatology and Clinical Immunology, University of Florida, Gainesville, FL 32610; †Center for Autoimmune Disease, University of Florida, Gainesville, FL 32610; ‡Laboratory of Host Defense, WPI Immunology Frontier Research Center, Osaka University, Osaka 565-0871, Japan; and §Department of Pathology, Immunology and Laboratory Medicine, University of Florida, Gainesville, FL 32610

[1]P.Y.L. and Y.K. contributed equally to this work.

Received for publication April 22, 2010. Accepted for publication November 23, 2010.

This work was supported by Grant R01-AR44731 from the U.S. Public Health Service, a grant from the Lupus Research Institute, and by generous gifts from Lupus Link, Inc. (Daytona Beach, FL) and Mr. Lewis M. Schott to the University of Florida Center for Autoimmune Disease. P.Y.L was a National Institutes of Health T32 trainee (DK07518).

Address correspondence and reprint requests to Dr. Westley Reeves, Division of Rheumatology and Clinical Immunology, University of Florida, P.O. Box 100221, Gainesville, FL 32610-0221. E-mail address: whreeves@ufl.edu

The online version of this article contains supplemental material.

Abbreviations used in this article: ASC, apoptosis-associated speck-like protein containing a caspase recruitment domain; IFN-I, type I IFN; IRAK, IL-1R–associated kinase; IRF-7, IFN regulatory factor-7; PEC, peritoneal exudate cell; Q-PCR, quantitative PCR; TMPD, 2,6,10,14 tetramethylpentadecane.

www.jimmunol.org/cgi/doi/10.4049/jimmunol.1001328

like protein containing a caspase recruitment domain (ASC)$^{-/-}$, Nalp3$^{-/-}$, caspase-1$^{-/-}$, IL-1R–associated kinase (IRAK-1)$^{-/-}$, IRAK-2$^{-/-}$, IRAK-1$^{-/-}$IRAK-2$^{-/-}$, IRAK-4$^{-/-}$, and IFN regulatory factor-7 (IRF-7)$^{-/-}$ mice (on a C57BL/6 background), and littermate controls were bred and maintained in a specific pathogen-free facility at Osaka University. Mice (8–10-wk-old) received 0.5 ml i.p. injection of TMPD, pentadecane, *n*-hexadecane, squalene (Sigma-Aldrich, St. Louis, MO), or mineral oil (Harris Teeter, Matthews, NC). Peripheral blood and peritoneal exudate cells (PECs) were isolated as described (9). For morphological analysis, neutrophils were sorted using PE-conjugated anti-Ly6G and magnetic bead-conjugated anti-PE Abs (17). Fifty thousand sorted cells were cytocentrifuged onto glass slides (Fisher Scientific, Pittsburgh, PA) and stained using the Hema3 kit (Fisher Scientific). For IL-1α and CXCL5 blockade, mice treated with TMPD for 2 wk were given 200 μg anti–IL-1α neutralizing Abs, hamster IgG (Biolegend, San Diego, CA), anti-CXCL5 neutralizing Abs, or rat IgG1 isotype control Abs (R&D Systems, Minneapolis, MN) i.p., and analysis was performed after 24 h.

Real-time quantitative PCR

Quantitative PCR (Q-PCR) was performed as previously described (17). Briefly, total RNA was extracted from 10^6 peritoneal cells using TRIzol (Invitrogen, Carlsbad, CA), and cDNA was synthesized using the Superscript II First-Strand Synthesis Kit (Invitrogen). Q-PCR was performed using the SYBR Green JumpStart Kit (Sigma-Aldrich) with an Opticon II thermocycler (Bio-Rad, Hercules, CA). Amplification conditions were: 95°C for 10 min, followed by 45 cycles of 94°C for 15 s, 60°C for 25 s, and 72°C for 25 s. After the final extension (72°C for 10 min), a melting-curve analysis was performed to ensure specificity of the products. Gene expression was normalized to 18S RNA, and expression relative to the sample with the lowest expression was calculated using the $2^{-\Delta\Delta Ct}$ method (18). Primers used in this study were all described previously (15, 16) except for CXCL2 (forward: 5′-AAGTTTGCCTTGACCCTGAA-3′; reverse: 5′-CGAGGCACATCAGGTACGAT-3′) and CXCL3 (5′-forward: CCACTCTCAAGGATGGTCAA-3′; reverse: 5′-GGATGGATCGCTTTTCTCTG-3′).

Flow cytometry

The following conjugated Abs were used: anti–CD11b-PE, anti–CD8-allophycocyanin, anti–CD4-FITC, anti–CD11c-PE, anti–B220-allophycocyanin–Cy5.5, anti–Ly6G-PE, anti–Ly6C-FITC, anti–Ly6C-biotin, anti–Siglec-F–biotin (all from BD Biosciences, San Jose, CA), anti–CCR3-Alexa 647, anti–CD11b-Pacific Blue (Biolegend), and avidin-allophycocyanin (eBioscience, San Diego, CA). Cells were then stained with an optimized amount of primary Abs or the appropriate isotype control for 10 min at room temperature as previously described (15). Fifty thousand events per sample were acquired using a CYAN ADP flow cytometer (Beckman Coulter, Hialeah, FL) and analyzed with FCS Express 3 (De Novo Software, Ontario, Canada).

ELISA

CXCL1, CXCL2 (PeproTech, Rocky Hill, NJ), and CXCL5 ELISA (R&D Systems) were performed following the manufacturer's instructions. OD was converted to concentration using standard curves based on recombinant chemokines analyzed by a four-parameter logistic equation (Softmax Pro 4.3; Molecular Devices, Sunnyvale, CA).

Cell culture

NIH3T3 cells were cultured in complete DMEM (containing 10% FBS, 10 mM HEPES, glutamine, penicillin/streptomycin, and 10 U/ml heparin) and seeded on 24-well cell-culture plates (10^5 cells/well). Cells were stimulated with PBS or 500 pg/ml rIL-1α (Biolegend), IL-1β (BD Bioscience), or IFN-β (PBL Laboratories, Piscataway, NJ) and incubated at 37°C in a 5% CO_2 atmosphere for 6 h. RNA extraction and Q-PCR were performed as described above.

Statistical analysis

For quantitative variables, differences between groups were analyzed by the unpaired Student *t* test. Data are presented as mean ± SE. All tests were two-sided. A p value <0.05 was considered significant. Statistical analyses were performed using Prism 4.0 (GraphPad Software, San Diego, CA).

Results

Chronic recruitment of neutrophils induced by TMPD and other hydrocarbons

The inflammatory response to TPMD is characterized by chronic accumulation of monocytes and neutrophils in the peritoneal cavity (8). To better understand the mechanism of neutrophil recruitment in this model, we first studied the time course of neutrophil accumulation. In untreated or PBS-treated wild-type C57BL/6 mice, very few neutrophils (characterized by surface expression of the myeloid marker CD11b and the neutrophil-specific marker Ly6G) were present in the peritoneal cavity (Fig. 1*A*). Neutrophils begin to accumulate within 24 h of TMPD treatment, comprising about one third of the PECs (Fig. 1*A*). The absolute number of neutrophils peaked after 2 wk and remained stable for 4–6 wk before a gradual decline was observed (Fig. 1*B* and data not shown). Magnetic bead sorting of PECs using Abs to Ly6G yielded polymorphonuclear cells morphologically consistent with neutrophils (Fig. 1*C*). Based on these findings, all subsequent analyses were performed 2 wk after TMPD treatment. Nevertheless, neutrophils were detectable up to 6 mo post TMPD treatment (Fig. 1*A*, 1*B*), illustrating the chronicity of the inflammatory response. The infiltration of eosinophils, which are distinguished from neutrophils by morphology and surface expression of CCR3 and Siglec-F (19), was minimal in TMPD-treated mice (Supplemental Fig. 1).

In addition, an expansion of the neutrophil compartment in the peripheral blood also was evident following TMPD treatment. Whereas small numbers of inflammatory monocytes displaying high surface expression of Ly6C and no expression of Ly6G were seen in the peripheral blood of untreated mice (Fig. 1*D*, ovals), larger numbers of neutrophils expressing intermediate levels of Ly6C (boxes) in addition to Ly6G were present. Two weeks after TMPD injection, the proportions of both Ly6C^{hi} monocytes and neutrophils in the peripheral blood were increased by 2–3-fold compared with baseline levels (Fig. 1*D*).

These changes were not strain specific, as neutrophil influx was also detected in other wild-type strains injected with TMPD, although the greatest effect was seen in BALB/c mice (Table I). Furthermore, we extended our analysis to other naturally occurring hydrocarbons including mineral oil, squalene, pentadecane, and *n*-hexadecane. Similar to TMPD, all of these hydrocarbons elicited chronic recruitment of neutrophils into the peritoneal cavity (Fig. 1*E*). This number of neutrophils in PECs 2 wk after mineral oil or squalene treatment was similar to TMPD, whereas hexadecane or pentadecane treatment elicited slightly greater levels of neutrophils.

TMPD-induced neutrophil recruitment is mediated by IL-1R signaling

The mechanism of hydrocarbon-induced chronic neutrophil recruitment remains unclear and appears independent of the pathways required for monocyte migration. Recent studies demonstrated that although TLR-7, IFN-I receptor, and CCR2 are essential for the persistent recruitment of Ly6C^{hi} monocytes into the peritoneal cavity following TMPD treatment, these components are all dispensable for the neutrophil response (15, 16). To identify the mechanism(s) responsible for the chronic neutrophil influx, we first examined the role of several proinflammatory mediators previously implicated in the immune response to TMPD (9, 10, 17, 20). Compared to wild-type controls, mice deficient in TNF-α or FcR γ-chain all showed comparable levels of neutrophil recruitment 2 wk after TMPD injection. The response was also similar in C3H/HeJ mice, suggesting that endotoxin is not responsible for our observations (Fig. 2*A*). Moreover, the infiltration of neutrophils in this model was not dependent on Nalp3/cryopyrin, ASC, or caspase-1 (Fig. 2*B*). These components of the inflammasome complex are key mediators of neutrophil migration in several models of sterile inflammation (21–23).

Interestingly, the accumulation of neutrophils in the peritoneal cavity was largely abolished in the absence of IL-1R type I (Fig.

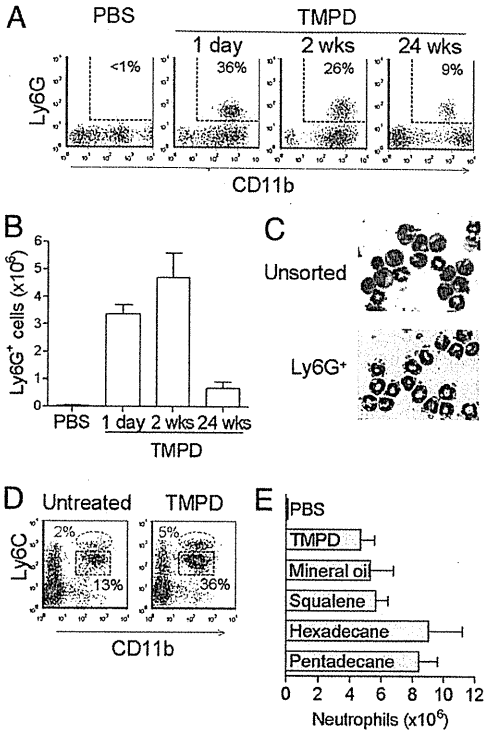

FIGURE 1. TMPD induces chronic recruitment of neutrophils in mice. Flow cytometry (*A*) and quantification of PECs (*B*) in wild-type C57BL/6 mice treated with PBS or TMPD at the indicated time points after treatment ($n = 4$ per group). Neutrophils are characterized by coexpression of CD11b and Ly6G. The percentage of neutrophils is indicated within each plot. *C*, Morphologic analysis of PECs from TMPD-treated mice before and after magnetic bead sorting using anti-Ly6G Abs (original magnification ×200). *D*, Flow cytometry of peripheral blood cells in C57BL/6 mice before and 2 wk after TMPD treatment. Dotted ovals indicate $Ly6C^{hi}$ monocytes ($CD11b^+Ly6C^{hi}$) and boxes indicate neutrophils ($CD11b^+Ly6C^{mid}$). The percentage of both populations is indicated within each plot. *E*, Quantification of PECs in C57BL/6 mice treated with PBS or various hydrocarbon oils for 2 wk ($n = 4$ per group). For bar graphs, each bar represents the mean and error bars indicate SE.

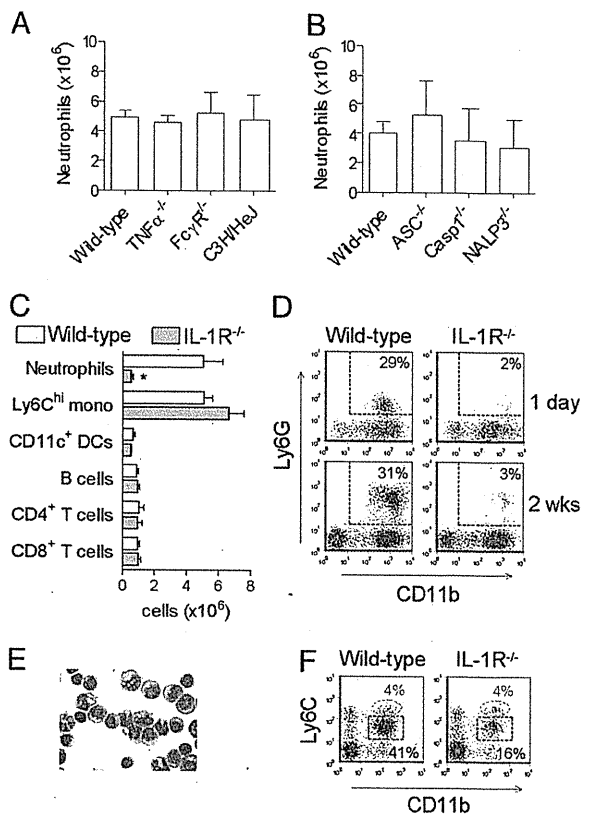

FIGURE 2. TMPD-induced neutrophil recruitment is mediated by IL-1R signaling. *A*, Quantification of $Ly6G^+$ neutrophils in PECs from TMPD-treated wild-type C57BL/6, TNF-$\alpha^{-/-}$, FcRγ-chain$^{-/-}$, and C3H/HeJ mice ($n = 6$ to 7 per group). *B*, Quantification of $Ly6G^+$ neutrophils in PECs from TMPD-treated C57BL/6, $ASC^{-/-}$, caspase-$1^{-/-}$, and $NALP3^{-/-}$ mice ($n = 8$ per group). *C*, Comparison of PEC populations in TMPD-treated C57BL/6 and IL-$1R^{-/-}$ mice ($n = 6$ per group). *D*, Flow cytometry of PECs from C57BL/6 and IL-$1R^{-/-}$ mice 1 d or 2 wk after TMPD treatment. The percentage of neutrophils is indicated within each plot. *E*, Morphologic analysis of PECs from TMPD-treated IL-$1R^{-/-}$ mice (original magnification ×200). *F*, Flow cytometry of peripheral blood cells in TMPD-treated C57BL/6 and IL-$1R^{-/-}$ mice. Dotted ovals indicate $Ly6C^{hi}$ monocytes ($CD11b^+Ly6C^{hi}$), and boxes indicate neutrophils ($CD11b^+Ly6C^{mid}$). The percentages of cells in these populations are indicated within each plot. For all panels, unless otherwise noted, all mice were treated with TMPD 2 wk prior to analysis. Each bar in bar graphs represents the mean and error bars indicate SE. $^*p < 0.05$ compared with wild-type controls (Student's unpaired *t* test).

2*C*). This effect was specific as numbers of $Ly6C^{hi}$ monocytes, B lymphocytes, T lymphocytes, and dendritic cells in the peritoneal exudate were comparable to wild-type mice. The depletion of neutrophils was evident at 1 d or 2 wk post TMPD treatment, indicating that IL-1R signaling mediates both acute and chronic neutrophil recruitment in this model (Fig. 2*D*). Consistent with these findings, morphological analysis of PECs from TMPD-treated IL-$1R^{-/-}$ mice showed a predominance of monocytes and lymphocytes, whereas few neutrophils were present (Fig. 2*E*). Moreover, expansion of the neutrophil compartment in the peripheral blood also was abrogated in the absence of IL-1R (Fig. 2*F*). These data suggest that neutrophil recruitment in the TMPD model of chronic inflammation is specifically mediated by IL-1R signaling.

Table I. Quantification of peritoneal exudate cells in wild-type mouse strains 2 wk after TMPD treatment

Strain	*n*	Neutrophils	$Ly6C^{hi}$ Monocytes	Dendritic Cells	B Cells	$CD4^+$ T Cells	$CD8^+$ T Cells
C57BL/6	6	4.32 ± 0.60	4.80 ± 0.87	0.50 ± 0.07	0.85 ± 0.23	0.90 ± 0.27	0.90 ± 0.23
BALB/cJ	6	9.49 ± 0.43	2.36 ± 0.15	0.23 ± 0.02	0.68 ± 0.05	0.64 ± 0.11	1.13 ± 0.18
129/Sv	6	3.23 ± 0.54	4.85 ± 0.48	0.31 ± 0.08	0.84 ± 0.20	1.03 ± 0.17	0.79 ± 0.14
C3H/OuJ	6	4.80 ± 1.60	4.50 ± 1.58	0.35 ± 0.07	0.90 ± 0.26	0.35 ± 0.07	0.23 ± 0.06
CBA/CaJ	4	3.37 ± 0.38	3.65 ± 1.04	0.27 ± 0.07	0.83 ± 0.24	1.20 ± 0.15	0.37 ± 0.03

All values represent cell number × 10^6. Cell populations were quantified by flow cytometry using the following surface markers: neutrophils ($CD11b^+$ $Ly6G^+$), $Ly6C^{hi}$ monocytes ($CD11b^+Ly6C^{hi}$), dendritic cells ($CD11C^+I^A/I^{E+}$), B lymphocytes ($B220^+CD11C^-$), $CD4^+$ T cells ($CD4^+CD11C^-CD11b^-$) and $CD8^+$ T cells ($CD8^+CD11C^-CD11b^-$).

MyD88 and IRAKs modulate both monocyte and neutrophil recruitment

To elucidate the pathway downstream of IL-1R, we tested the effects of TMPD in mice deficient of the adaptor molecules involved in IL-1R signaling including MyD88 and members of the IRAK family (24–26). Consistent with the essential role of MyD88 and IRAK-4 in IL-1R signaling, the number of neutrophils in the peritoneal cavity after TMPD treatment was significantly reduced in the absence of these molecules (Fig. 3*A*). Unlike IL-1R$^{-/-}$ mice, which demonstrated normal recruitment of Ly6C^{hi} monocytes (Fig. 2*C*), TMPD-treated IRAK-4$^{-/-}$ mice exhibited a drastic reduction of these inflammatory monocytes in the peritoneal cavity (Fig. 3*B*). As described previously (15), this also was seen in MyD88-deficient mice. In the absence of significant monocyte and neutrophil influx, the total number of PECs was reduced by >90% in MyD88$^{-/-}$ and IRAK-4$^{-/-}$ mice compared with wild-type mice (not shown).

IRAK-1 and IRAK-2 differentially regulate the signaling cascade downstream of IRAK-4 (27). Curiously, the recruitment of neutrophils was partially intact in the absence of either of these kinases (Fig. 3*B*). Combined deficiency of IRAK-1 and IRAK-2 was required to recapitulate the observations in IRAK-4$^{-/-}$ mice, suggesting that IRAK-1 and IRAK-2 can partially compensate for one another in the inflammatory response to TMPD.

Although the mechanisms of monocyte and neutrophil recruitment both require MyD88 and IRAKs, these pathways can be distinguished by downstream utilization of IRF-7. IRF-7 interacts with MyD88 and IRAKs to promote TLR-induced IFN-I production but does not participate in IL-1R signaling (28, 29). Consistent with requirement of TLR-7 activation and IFN-I production for monocyte recruitment (15, 16), IRF-7 deficiency resulted in defective accumulation of Ly6C^{hi} monocytes, but not neutrophils, following TMPD treatment (Fig. 3*A*, 3*B*). Taken together, these data suggest that IL-1R signaling specifically mediates neutrophil influx, whereas the adaptor molecule MyD88 and IRAKs 1/2/4 are shared with the pathway used for monocyte recruitment.

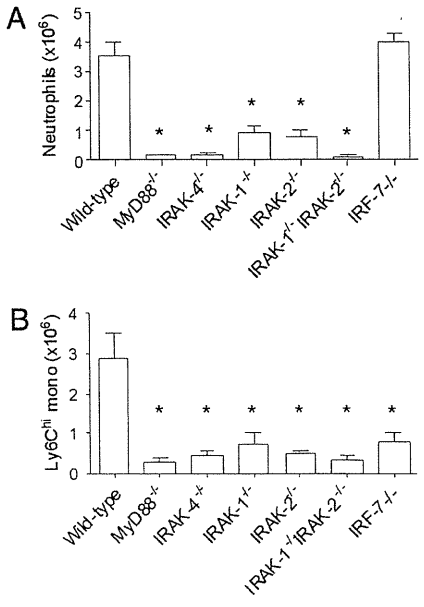

FIGURE 3. MyD88 and IRAK-4 mediate the recruitment of both neutrophils and inflammatory monocytes induced by TMPD. Quantification of neutrophils (*A*) and Ly6C^{hi} monocytes (*B*) in PECs from wild-type C57BL/6 (n = 7), MyD88$^{-/-}$ (n = 6), IRAK-4$^{-/-}$ (n = 8), IRAK-1$^{-/-}$ (n = 8), IRAK-2$^{-/-}$ (n = 8), IRAK-1$^{-/-}$ IRAK-2$^{-/-}$ (n = 6), and IRF-7$^{-/-}$ (n = 9) mice 2 wk after TMPD treatment. Each bar represents the mean, and error bars indicate SE. *$p < 0.05$ compared with wild-type controls (Student's unpaired t test).

IL-1α, but not IL-1β, is responsible for the influx of neutrophils

Because the IL-1R mediates responses to both IL-1α and IL-1β, we next evaluated the role of these cytokines in TMPD-treated mice. Compared to wild-type controls, IL-1β–deficient mice exhibited comparable levels of neutrophil recruitment 2 wk after TMPD injection (Fig. 4*A*, 4*B*). In line with these findings, the absence of caspase-1, a protease that generates the active form of IL-1β, did not impact the neutrophil response (Fig. 2*B*). To address the role of IL-1α, we tested the effects of monoclonal neutralizing Abs against IL-1α in mice treated with TMPD. A single dose of anti–IL-1α Abs reduced the infiltration of neutrophils by ~40–50% (Fig. 4*C*, 4*D*). This effect was specific to neutrophils as the numbers of monocytes and lymphocytes in the peritoneal cavity were not affected (data not shown). Therefore, IL-1α is the primary mediator of neutrophil influx in this model.

IL-1α promotes neutrophil recruitment by inducing CXCL5 expression

To further understand the mechanism of neutrophil migration driven by IL-1α, we studied the involvement of chemokines downstream of IL-1R signaling. Several members of the CXC chemokine family are potent neutrophil chemoattractants produced in response to IL-1R stimulation (30–32). In vitro studies using cultured fibroblasts showed that IL-1α and IL-1β are equally

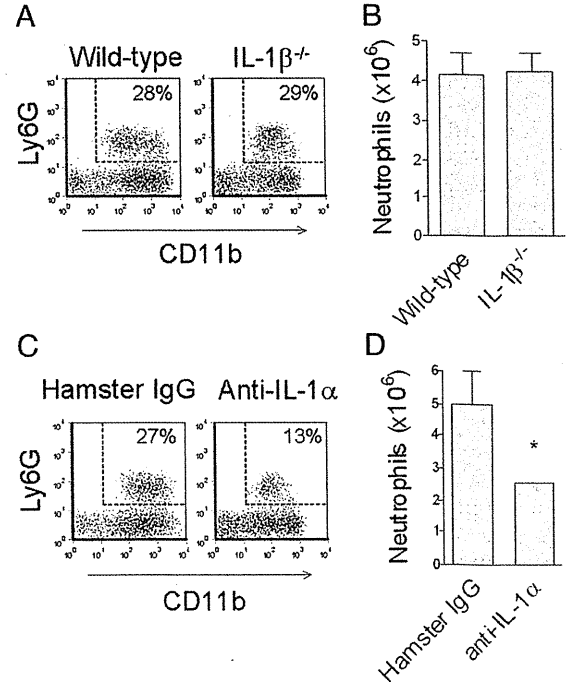

FIGURE 4. TMPD-induced neutrophil recruitment requires IL-1α, but not IL-1β. Flow cytometry (*A*) and quantification of neutrophils (*B*) in wild-type C57BL/6 and IL-1β$^{-/-}$ mice 2 wk after TMPD treatment (n = 7 per group). Flow cytometry (*C*) and quantification of neutrophils (*D*) in C57BL/6 mice injected with 200 μg hamster IgG or anti–IL-1α Abs 2 wk after TMPD treatment (n = 5 per group). Analysis was performed 24 h after Ab treatment. For all flow cytometry plots, the percentage of neutrophils is indicated within each plot. Each bar in bar graphs represents the mean, and error bars indicate SE. *$p < 0.05$ compared with wild-type or isotype controls (Student's unpaired t test).

effective in upregulating the transcription of the neutrophil chemoattractants CXCL1 and CXCL5 (Supplemental Fig. 2). In PECs from TMPD-treated mice, expression of the neutrophil chemoattractants CXCL1, CXCL2, CXCL3, and CXCL5 as well as the monocyte chemoattractants CCL2, CCL12, and CX_3CL1 all were detectable using Q-PCR (Fig. 5*A*). However, the transcript levels of CXCL5 were reduced significantly in IL-1R–deficient mice compared with wild-type controls, whereas the expression of other CXC chemokines and monocyte chemoattractants was largely unaffected. Supporting these findings, CXCL5 protein was readily detectable in the peritoneal lavage fluid at 1 d, 2 wk, and 1 mo post TMPD treatment (Fig. 5*B*). CXCL5 levels were drastically reduced in the peritoneal lavage fluid from TMPD-treated IL-$1R^{-/-}$ mice (Fig. 5*C*), whereas deficiency of IL-1β did not impact the production of this chemokine. The expression of CXCL5, but not CXCL1, CXCL2, or CXCL3, was similarly reduced by the administration of anti–IL-1α Abs (Fig. 5*D*). IL-1α blockade also reduced CXCL5 protein levels in the peritoneal lavage fluid (Fig. 5*E*).

In contrast to CXCL5, the amounts of CXCL1 in the peritoneal lavage fluid from TMPD-treated mice were small (Fig. 5*F*). Interestingly, although significant amounts of CXCL2 were detected in the lavage fluid, the production of this chemokine is intact in the absence of IL-1R (Fig. 5*G*). Because IL-1 signaling is responsible for ~90% of neutrophil influx both acutely and chronically after TMPD treatment (Fig. 2*D*), CXCL2 is unlikely to be the major neutrophil chemoattractant in this model.

To further evaluate whether CXCL5 is critical to neutrophil migration in this model, we tested the effect of TMPD in mice deficient of CXCR2, the primary receptor for CXCL5. Compared to wild-type BALB/c controls, $CXCR2^{-/-}$ mice exhibited ~90% reduction of neutrophil influx to the peritoneal cavity in response to TMPD treatment, recapitulating the observations in IL-$1R^{-/-}$ mice (Fig. 5*H*, 5*I*). Finally, we investigated the effect of CXCL5 blockade on granulocyte recruitment. Administration of neutralizing Abs to CXCL5 reduced the infiltration of granulocytes to the peritoneal cavity by ~30% compared with treatment with isotype control Abs (Fig. 5*J*). Taken together, these data suggest that IL-1α and IL-1R signaling promotes the chronic infiltration of granulocytes at least in part by inducing CXCL5 expression (Fig. 6).

Discussion

The proinflammatory effects of naturally occurring hydrocarbon oils were described more than a half century ago (7). These properties have been applied to the development of vaccines, in which hydrocarbons are commonly incorporated as adjuvants to augment the response to immunization (6, 7). In contrast, exposure to hydrocarbons is associated with the development of chronic inflammation and a variety of pathological findings including plasmacytoma formation, lymphoid neogenesis, and autoimmune manifestations (2–5). The mechanism(s) of hydrocarbon-induced inflammation remains largely unexplained.

TMPD is a medium-length hydrocarbon that elicits a potent chronic inflammatory response in mice characterized by persistent infiltration of neutrophils and monocytes (8). In this study, we illustrate the essential role of IL-1α in TMPD-induced neutrophil recruitment. IL-1α activates a pathway that requires IL-1R, MyD88, IRAK1/2, and IRAK-4, leading to a signaling cascade that culminates in the production of the neutrophil chemoattractant CXCL5 (Fig. 6). Blockade of IL-1α reduced the production of CXCL5 and infiltration of neutrophils to the peritoneal cavity in TMPD-treated mice. In contrast, neutrophil influx was

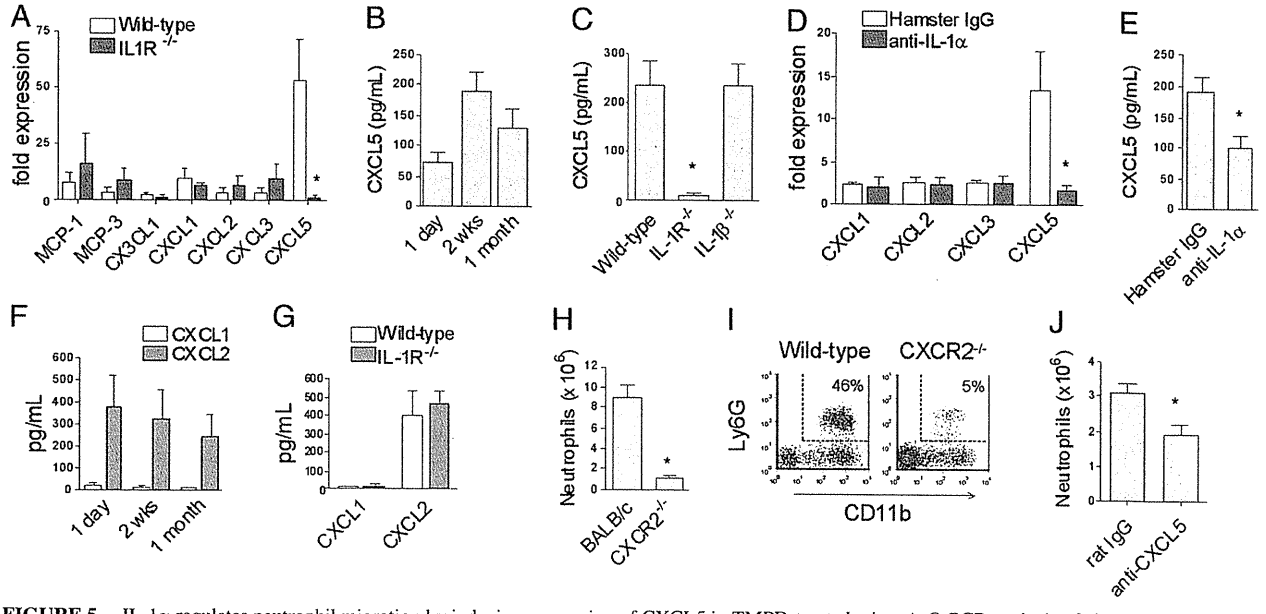

FIGURE 5. IL-1α regulates neutrophil migration by inducing expression of CXCL5 in TMPD-treated mice. *A*, Q-PCR analysis of chemokine expression in PECs from TMPD-treated C57BL/6 ($n = 5$) and IL-$1R^{-/-}$ mice ($n = 6$). ELISA quantification of CXCL5 in peritoneal lavage fluid from C57BL/6 mice treated with TMPD (*B*) for the indicated duration ($n = 4$ to 5 per group) and C57BL/6 ($n = 5$), IL-$1R^{-/-}$ ($n = 6$), and IL-$1\beta^{-/-}$ mice ($n = 4$) (*C*) 2 wk after TMPD treatment. *D*, Q-PCR analysis of chemokine expression in PECs from TMPD-treated wild-type C57BL/6 mice injected with 200 μg hamster IgG or anti–IL-1α Abs ($n = 5$ per group). *E*, ELISA quantification of CXCL5 in peritoneal lavage fluid from TMPD-treated C57BL/6 mice injected with hamster IgG or anti–IL-1α Abs ($n = 5$ per group). ELISA quantification of CXCL1 and CXCL2 in peritoneal lavage fluid from C57BL/6 mice treated with TMPD (*F*) for the indicated duration ($n = 4$ to 5 per group) and C57BL/6 ($n = 5$) and IL-$1R^{-/-}$ ($n = 6$) (*G*) 2 wk after TMPD treatment. Quantification (*H*) and flow cytometry analysis (*I*) of neutrophils in wild-type BALB/c and $CXCR2^{-/-}$ mice after TMPD treatment ($n = 7$ per group). *J*, Quantification of neutrophils in C57BL/6 mice injected with 200 μg anti-CXCL5 Abs or isotype control IgG1 2 wk after TMPD treatment ($n = 5$ per group). Unless otherwise indicated, all mice were treated with TMPD 2 wk prior to analysis. Each bar represents the mean and error bars indicate SE. $^*p < 0.05$ compared with wild-type or isotype controls (Student's unpaired *t* test).

not impacted by the absence of other proinflammatory mediators including IL-1β, TNF-α, IL-6, and TLR-4. Both IFN-γ and IFN-I are also dispensable (16). This mechanism is also different from the pathway used in chronic monocyte recruitment in the TMPD model (15, 16). The persistent influx of monocytes is mediated by the production of several CC-chemokines downstream of TLR-7 activation and IFN-I production (Fig. 6). Interestingly, the IL-1R and TLR signaling cascades share key signaling molecules including MyD88 and IRAK-4 (24–26). As a result, the recruitment of both neutrophils and monocytes is abolished in the absence of these molecules. These pathways diverge downstream of IRAK signaling. IFN-I production and monocyte recruitment initiated by TLR-7 depend on the transcription factor IRF-7, whereas IL-1R signaling and neutrophil recruitment is IRF-7 independent and likely mediated by NF-κB activation (33, 34).

How TMPD triggers the release of IL-1α remains to be solved. Recent evidence suggests that dying cells and cellular debris from the chronic inflammatory response may contribute to the release of this cytokine. Introduction of necrotic cells to the peritoneal cavity triggers neutrophil migration in an IL-1α–dependent manner (35). Interestingly, the release of IL-1α during necrosis, but not apoptosis, distinguishes the inflammatory response to the two types of cell death (36). Furthermore, necrotic cell debris is also a source of RNA-associated autoantigens (such as components of small ribonucleoproteins) (37–39), which may be responsible for the activation of TLR-7 and subsequent recruitment of Ly6C^{hi} monocytes in this model (Fig. 6). The target(s) of IL-1α is also not completely understood. Although gene expression data in PECs suggest a role of these inflammatory cells in the production of neutrophil chemoattractants, mesothelial cells also could be a major source of these chemokines. A recent study demonstrates that IL-1α released from dying cells stimulates the migration of neutrophils by inducing CXCL1 expression by mesothelial cells (40). Although a similar mechanism may be involved in TMPD-induced chronic inflammation, CXCL5 rather than CXCL1 seems to play a more prominent role in TMPD-induced neutrophil recruitment. Additional studies will be needed to distinguish the roles of mesothelial cells and PECs in this model.

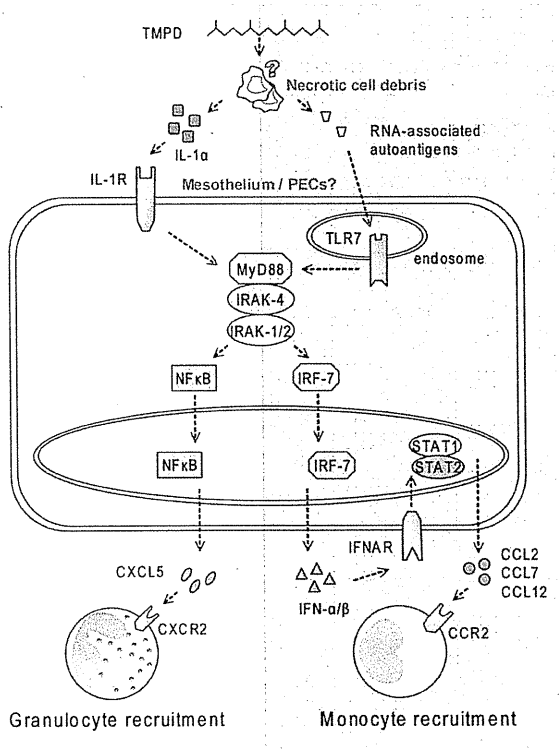

FIGURE 6. Proposed pathways of neutrophil and monocyte recruitment in TMPD-induced chronic inflammation. Neutrophil pathway (*left side*): TMPD treatment results in the release of IL-1α, likely from necrotic cells. In target cells such as mesothelial cells or peritoneal exudate cells, IL-1α stimulates the IL-1R complex, which initiates a signaling cascade that requires MyD88 and IRAKs, culminating in the activation of NF-κB and production of the neutrophil chemoattractant CXCL5. Neutrophils migrate to CXCL5 via a CXCR2-dependent mechanism. Monocyte pathway (*right side*): TMPD treatment results in the activation of TLR-7, which elicits the production of IFN-I through a MyD88- and IRAK-4–dependent pathway. IFN-I binds to IFNAR and subsequent signaling events result in the production of IFN-stimulated chemokines including CCL2, CCL7, and CCL2. These chemokines mediate the migration of Ly6C^{hi} monocytes through their interaction with CCR2.

In addition to modulating chemokine production, IL-1α and IL-1R signaling possess other functions that may fuel the chronic inflammatory response. Transgenic overexpression of IL-1α in mice is sufficient to trigger a form of arthritis characterized by a predominance of macrophages and neutrophils in the synovium (41). As TMPD-treated BALB/c mice develop an inflammatory arthritis (42), it will be of interest to examine the effect of IL-1R deficiency on the pathogenesis of arthritis in this model. IL-1α also is thought to be responsible for the maintenance of granulopoiesis through the induction of neutrophil–M-CSF expression (41, 43). Indeed, the proliferation of not only neutrophil/macrophage progenitors, but also multipotent progenitors and hematopoietic stem cells, is supported by IL-1R signaling (44). This chemokine-independent mechanism may be responsible for the peripheral granulocytosis in TMPD-treated mice, although the effects of TMPD on the different progenitor populations have not been assessed.

CXCL5, also known as epithelial cell-derived neutrophil attractant 78, directs the migration of neutrophils primarily via the receptor CXCR2 (45, 46). The interaction between CXCL5 and CXCR2 is critical for neutrophil recruitment in several models of inflammatory disease (47–50). CXCL5 expression is induced by IL-1α, IL-1β, and TNF-α through activation of NF-κB (51–54), whereas IFN-α and IFN-γ both suppress the production of this chemokine (55, 56). Production of CXCL5 downstream of kinin B1 receptor activation plays an important role in IL-1β–induced neutrophil migration (57). Interestingly, CXCL5 is also a mediator of neutrophil migration in the inflammatory response induced by IL-23 and IL-17 (58). Although our data suggest that IL-1α is responsible for CXCL5 production in the TMPD model, whether the IL-23–IL-17 axis modulates IL-1α or CXCL5 expression warrants further investigation. It is noteworthy that our observations are also distinct from the inflammatory response to turpentine oil, which relies on IL-β production (59, 60). Furthermore, the monocyte chemoattractant CCL2 has been implicated in the chronic infiltration of neutrophils in a model of adjuvant-induced vasculitis (61). The involvement of CCL2 and its receptor CCR2, however, seems limited to the regulation of monocyte migration in mice exposed to i.p. TMPD.

A potential limitation of the current study is the partial response exhibited by IL-1α and CXCL5 blockade. Whereas the influx of neutrophils was inhibited by >90% in IL-1R$^{-/-}$ and CXCR2$^{-/-}$ mice, neutralization of IL-1α or CXCL5 only achieved a reduction of 30–40%. This level of response is comparable to another study that administered these Abs i.p (35, 58). Although the partial response is likely due to the unremitting inflammatory response to TMPD and/or the presence of neutrophils in the peritoneal cavity prior to administration of Abs, it remains possible that other

cofactors are involved. For example, IL-1 signaling can directly activate the vascular endothelium to augment neutrophil chemotaxis (62).

In conclusion, our study elucidates the molecular pathway responsible for neutrophil recruitment in hydrocarbon-induced chronic inflammation. These findings highlight the role of IL-1α in maintaining persistent neutrophil recruitment to sites of inflammation at least in part by regulating CXCL5 production. In view of the induction of lupus by TMPD, the current data also may be of interest with regard to the recent evidence that proinflammatory neutrophils are involved in the pathogenesis of vascular disease in lupus patients (63). Whether therapeutic interventions targeting IL-1α, CXCL5, or CXCR2 are effective in chronic inflammatory or vascular diseases or in the inflammatory arthritis induced by TMPD warrants further evaluation.

Acknowledgments

We thank Dr. Vishva Dixit (Genentech, San Francisco, CA) for generously providing ASC$^{-/-}$, Nalp3$^{-/-}$, and caspase-1$^{-/-}$ mice, Drs. Nicolas Turrin (Laval University, Quebec, Canada), Scott Bercelli, and Kerry O'Malley (University of Florida) for generously providing IL-1β$^{-/-}$ mice, M. Kumagai, Y. Fujiwara, and A. Yoshimura for technical assistance, and E. Kamada for secretarial assistance. We also thank the Malcolm Randall Veterans Affairs Medical Center animal facility for assistance with animal husbandry.

Disclosures

The authors have no financial conflicts of interest.

References

1. Kumar, V., A. K. Abbas, N. Fausto, S. L. Robbins, and R. S. Cotran. 2004. Acute and Chronic Inflammation. In *Robbins & Cotran Pathologic Basis of Disease*, 7th Ed. V. Kumar, A. Abbas, and N. Fausto, eds. Elsevier Health Sciences, Philadephia, PA, p. 50–88.
2. Reeves, W. H., P. Y. Lee, J. S. Weinstein, M. Satoh, and L. Lu. 2009. Induction of autoimmunity by pristane and other naturally occurring hydrocarbons. *Trends Immunol.* 30: 455–464.
3. Spickard, A., III, and J. V. Hirschmann. 1994. Exogenous lipoid pneumonia. *Arch. Intern. Med.* 154: 686–692.
4. Satoh, M., and W. H. Reeves. 1994. Induction of lupus-associated autoantibodies in BALB/c mice by intraperitoneal injection of pristane. *J. Exp. Med.* 180: 2341–2346.
5. Anderson, P. N., and M. Potter. 1969. Induction of plasma cell tumours in BALB-c mice with 2,6,10,14-tetramethylpentadecane (pristane). *Nature* 222: 994–995.
6. Wilner, B. I., M. A. Evers, H. D. Troutman, F. W. Trader, and I. W. McLean. 1963. Vaccine Potentiation by Emulsification with Pure Hydrocarbon Compounds. *J. Immunol.* 91: 210–229.
7. Ehrich, W. E., S. P. Halbert, E. Mertens, and S. Mudd. 1945. Mechanism of the Augmenting Action of Mineral Oil on Antibody Production: Tissue Reactions and Antibody Response to Dysentery Vaccine in Saline, and in Saline-Lanolin-Mineral Oil Emulsion. *J. Exp. Med.* 82: 343–360.
8. Cancro, M., and M. Potter. 1976. The requirement of an adherent cell substratum for the growth of developing plasmacytoma cells in vivo. *J. Exp. Med.* 144: 1554–1567.
9. Nacionales, D. C., K. M. Kelly, P. Y. Lee, H. Zhuang, Y. Li, J. S. Weinstein, E. Sobel, Y. Kuroda, J. Akaogi, M. Satoh, and W. H. Reeves. 2006. Type I interferon production by tertiary lymphoid tissue developing in response to 2,6,10,14-tetramethyl-pentadecane (pristane). *Am. J. Pathol.* 168: 1227–1240.
10. Patten, C., K. Bush, I. Rioja, R. Morgan, P. Wooley, J. Trill, and P. Life. 2004. Characterization of pristane-induced arthritis, a murine model of chronic disease: response to antirheumatic agents, expression of joint cytokines, and immunopathology. *Arthritis Rheum.* 50: 3334–3345.
11. Satoh, M., K. J. Hamilton, A. K. Ajmani, X. Dong, J. Wang, Y. S. Kanwar, and W. H. Reeves. 1996. Autoantibodies to ribosomal P antigens with immune complex glomerulonephritis in SJL mice treated with pristane. *J. Immunol.* 157: 3200–3206.
12. Satoh, M., A. Kumar, Y. S. Kanwar, and W. H. Reeves. 1995. Anti-nuclear antibody production and immune-complex glomerulonephritis in BALB/c mice treated with pristane. *Proc. Natl. Acad. Sci. USA* 92: 10934–10938.
13. Chowdhary, V. R., J. P. Grande, H. S. Luthra, and C. S. David. 2007. Characterization of haemorrhagic pulmonary capillaritis: another manifestation of Pristane-induced lupus. *Rheumatology (Oxford)* 46: 1405–1410.
14. Hoogenraad, N., T. Helman, and J. Hoogenraad. 1983. The effect of pre-injection of mice with pristane on ascites tumour formation and monoclonal antibody production. *J. Immunol. Methods* 61: 317–320.
15. Lee, P. Y., Y. Kumagai, Y. Li, O. Takeuchi, H. Yoshida, J. Weinstein, E. S. Kellner, D. Nacionales, T. Barker, K. Kelly-Scumpia, et al. 2008. TLR7-dependent and FcgammaR-independent production of type I interferon in experimental mouse lupus. *J. Exp. Med.* 205: 2995–3006.
16. Lee, P. Y., Y. Li, Y. Kumagai, Y. Xu, J. S. Weinstein, E. S. Kellner, D. C. Nacionales, E. J. Butfiloski, N. van Rooijen, S. Akira, et al. 2009. Type I interferon modulates monocyte recruitment and maturation in chronic inflammation. *Am. J. Pathol.* 175: 2023–2033.
17. Lee, P. Y., J. S. Weinstein, D. C. Nacionales, P. O. Scumpia, Y. Li, E. Butfiloski, N. van Rooijen, L. Moldawer, M. Satoh, and W. H. Reeves. 2008. A novel type I IFN-producing cell subset in murine lupus. *J. Immunol.* 180: 5101–5108.
18. Livak, K. J., and T. D. Schmittgen. 2001. Analysis of relative gene expression data using real-time quantitative PCR and the 2(-Delta Delta C(T)) Method. *Methods* 25: 402–408.
19. Voehringer, D., N. van Rooijen, and R. M. Locksley. 2007. Eosinophils develop in distinct stages and are recruited to peripheral sites by alternatively activated macrophages. *J. Leukoc. Biol.* 81: 1434–1444.
20. Kuroda, Y., J. Akaogi, D. C. Nacionales, S. C. Wasdo, N. J. Szabo, W. H. Reeves, and M. Satoh. 2004. Distinctive patterns of autoimmune response induced by different types of mineral oil. *Toxicol. Sci.* 78: 222–228.
21. Franchi, L., T. Eigenbrod, R. Muñoz-Planillo, and G. Nuñez. 2009. The inflammasome: a caspase-1-activation platform that regulates immune responses and disease pathogenesis. *Nat. Immunol.* 10: 241–247.
22. Hornung, V., F. Bauernfeind, A. Halle, E. O. Samstad, H. Kono, K. L. Rock, K. A. Fitzgerald, and E. Latz. 2008. Silica crystals and aluminum salts activate the NALP3 inflammasome through phagosomal destabilization. *Nat. Immunol.* 9: 847–856.
23. Martinon, F., V. Pétrilli, A. Mayor, A. Tardivel, and J. Tschopp. 2006. Gout-associated uric acid crystals activate the NALP3 inflammasome. *Nature* 440: 237–241.
24. Suzuki, N., S. Suzuki, G. S. Duncan, D. G. Millar, T. Wada, C. Mirtsos, H. Takada, A. Wakeham, A. Itie, S. Li, et al. 2002. Severe impairment of interleukin-1 and Toll-like receptor signalling in mice lacking IRAK-4. *Nature* 416: 750–756.
25. Adachi, O., T. Kawai, K. Takeda, M. Matsumoto, H. Tsutsui, M. Sakagami, K. Nakanishi, and S. Akira. 1998. Targeted disruption of the MyD88 gene results in loss of IL-1- and IL-18-mediated function. *Immunity* 9: 143–150.
26. Muzio, M., J. Ni, P. Feng, and V. M. Dixit. 1997. IRAK (Pelle) family member IRAK-2 and MyD88 as proximal mediators of IL-1 signaling. *Science* 278: 1612–1615.
27. Kawagoe, T., S. Sato, K. Matsushita, H. Kato, K. Matsui, Y. Kumagai, T. Saitoh, T. Kawai, O. Takeuchi, and S. Akira. 2008. Sequential control of Toll-like receptor-dependent responses by IRAK1 and IRAK2. *Nat. Immunol.* 9: 684–691.
28. Honda, K., H. Yanai, H. Negishi, M. Asagiri, M. Sato, T. Mizutani, N. Shimada, Y. Ohba, A. Takaoka, N. Yoshida, and T. Taniguchi. 2005. IRF-7 is the master regulator of type-I interferon-dependent immune responses. *Nature* 434: 772–777.
29. Uematsu, S., S. Sato, M. Yamamoto, T. Hirotani, H. Kato, F. Takeshita, M. Matsuda, C. Coban, K. J. Ishii, T. Kawai, et al. 2005. Interleukin-1 receptor-associated kinase-1 plays an essential role for Toll-like receptor (TLR)7- and TLR9-mediated interferon-alpha induction. *J. Exp. Med.* 201: 915–923.
30. Groves, R. W., T. Rauschmayr, K. Nakamura, S. Sarkar, I. R. Williams, and T. S. Kupper. 1996. Inflammatory and hyperproliferative skin disease in mice that express elevated levels of the IL-1 receptor (type I) on epidermal keratinocytes. Evidence that IL-1-inducible secondary cytokines produced by keratinocytes in vivo can cause skin disease. *J. Clin. Invest.* 98: 336–344.
31. Tumpey, T. M., R. Fenton, S. Molesworth-Kenyon, J. E. Oakes, and R. N. Lausch. 2002. Role for macrophage inflammatory protein 2 (MIP-2), MIP-1alpha, and interleukin-1alpha in the delayed-type hypersensitivity response to viral antigen. *J. Virol.* 76: 8050–8057.
32. West-Mays, J. A., P. M. Sadow, T. W. Tobin, K. J. Strissel, C. Cintron, and M. E. Fini. 1997. Repair phenotype in corneal fibroblasts is controlled by an interleukin-1 alpha autocrine feedback loop. *Invest. Ophthalmol. Vis. Sci.* 38: 1367–1379.
33. Dinarello, C. A. 2009. Immunological and inflammatory functions of the interleukin-1 family. *Annu. Rev. Immunol.* 27: 519–550.
34. Leung, K., J. C. Betts, L. Xu, and G. J. Nabel. 1994. The cytoplasmic domain of the interleukin-1 receptor is required for nuclear factor-kappa B signal transduction. *J. Biol. Chem.* 269: 1579–1582.
35. Chen, C. J., H. Kono, D. Golenbock, G. Reed, S. Akira, and K. L. Rock. 2007. Identification of a key pathway required for the sterile inflammatory response triggered by dying cells. *Nat. Med.* 13: 851–856.
36. Cohen, I., P. Rider, Y. Carmi, A. Braiman, S. Dotan, M. R. White, E. Voronov, M. U. Martin, C. A. Dinarello, and R. N. Apte. 2010. Differential release of chromatin-bound IL-1alpha discriminates between necrotic and apoptotic cell death by the ability to induce sterile inflammation. *Proc. Natl. Acad. Sci. USA* 107: 2574–2579.
37. Barrat, F. J., T. Meeker, J. Gregorio, J. H. Chan, S. Uematsu, S. Akira, B. Chang, O. Duramad, and R. L. Coffman. 2005. Nucleic acids of mammalian origin can act as endogenous ligands for Toll-like receptors and may promote systemic lupus erythematosus. *J. Exp. Med.* 202: 1131–1139.
38. Lau, C. M., C. Broughton, A. S. Tabor, S. Akira, R. A. Flavell, M. J. Mamula, S. R. Christensen, M. J. Shlomchik, G. A. Viglianti, I. R. Rifkin, and A. Marshak-Rothstein. 2005. RNA-associated autoantigens activate B cells by combined B cell antigen receptor/Toll-like receptor 7 engagement. *J. Exp. Med.* 202: 1171–1177.

39. Vollmer, J., S. Tluk, C. Schmitz, S. Hamm, M. Jurk, A. Forsbach, S. Akira, K. M. Kelly, W. H. Reeves, S. Bauer, and A. M. Krieg. 2005. Immune stimulation mediated by autoantigen binding sites within small nuclear RNAs involves Toll-like receptors 7 and 8. *J. Exp. Med.* 202: 1575–1585.
40. Eigenbrod, T., J. H. Park, J. Harder, Y. Iwakura, and G. Núñez. 2008. Cutting edge: critical role for mesothelial cells in necrosis-induced inflammation through the recognition of IL-1 alpha released from dying cells. *J. Immunol.* 181: 8194–8198.
41. Niki, Y., H. Yamada, S. Seki, T. Kikuchi, H. Takaishi, Y. Toyama, K. Fujikawa, and N. Tada. 2001. Macrophage- and neutrophil-dominant arthritis in human IL-1 alpha transgenic mice. *J. Clin. Invest.* 107: 1127–1135.
42. Potter, M., and J. S. Wax. 1981. Genetics of susceptibility to pristane-induced plasmacytomas in BALB/cAn: reduced susceptibility in BALB/cJ with a brief description of pristane-induced arthritis. *J. Immunol.* 127: 1591–1595.
43. Stork, L. C., V. M. Peterson, C. H. Rundus, and W. A. Robinson. 1988. Interleukin-1 enhances murine granulopoiesis in vivo. *Exp. Hematol.* 16: 163–167.
44. Ueda, Y., D. W. Cain, M. Kuraoka, M. Kondo, and G. Kelsoe. 2009. IL-1R type I-dependent hemopoietic stem cell proliferation is necessary for inflammatory granulopoiesis and reactive neutrophilia. *J. Immunol.* 182: 6477–6484.
45. Corbett, M. S., I. Schmitt, O. Riess, and A. Walz. 1994. Characterization of the gene for human neutrophil-activating peptide 78 (ENA-78). *Biochem. Biophys. Res. Commun.* 205: 612–617.
46. Walz, A., R. Burgener, B. Car, M. Baggiolini, S. L. Kunkel, and R. M. Strieter. 1991. Structure and neutrophil-activating properties of a novel inflammatory peptide (ENA-78) with homology to interleukin 8. *J. Exp. Med.* 174: 1355–1362.
47. Grespan, R., S. Y. Fukada, H. P. Lemos, S. M. Vieira, M. H. Napimoga, M. M. Teixeira, A. R. Fraser, F. Y. Liew, I. B. McInnes, and F. Q. Cunha. 2008. CXCR2-specific chemokines mediate leukotriene B4-dependent recruitment of neutrophils to inflamed joints in mice with antigen-induced arthritis. *Arthritis Rheum.* 58: 2030–2040.
48. Halloran, M. M., J. M. Woods, R. M. Strieter, Z. Szekanecz, M. V. Volin, S. Hosaka, G. K. Haines, III, S. L. Kunkel, M. D. Burdick, A. Walz, and A. E. Koch. 1999. The role of an epithelial neutrophil-activating peptide-78-like protein in rat adjuvant-induced arthritis. *J. Immunol.* 162: 7492–7500.
49. Colletti, L. M., S. L. Kunkel, A. Walz, M. D. Burdick, R. G. Kunkel, C. A. Wilke, and R. M. Strieter. 1995. Chemokine expression during hepatic ischemia/reperfusion-induced lung injury in the rat. The role of epithelial neutrophil activating protein. *J. Clin. Invest.* 95: 134–141.
50. Koch, A. E., S. L. Kunkel, L. A. Harlow, D. D. Mazarakis, G. K. Haines, M. D. Burdick, R. M. Pope, A. Walz, and R. M. Strieter. 1994. Epithelial neutrophil activating peptide-78: a novel chemotactic cytokine for neutrophils in arthritis. *J. Clin. Invest.* 94: 1012–1018.
51. Fillmore, R. A., S. E. Nelson, R. N. Lausch, and J. E. Oakes. 2003. Differential regulation of ENA-78 and GCP-2 gene expression in human corneal keratocytes and epithelial cells. *Invest. Ophthalmol. Vis. Sci.* 44: 3432–3437.
52. Chang, M. S., J. McNinch, R. Basu, and S. Simonet. 1994. Cloning and characterization of the human neutrophil-activating peptide (ENA-78) gene. *J. Biol. Chem.* 269: 25277–25282.
53. Lee, Y. R., S. H. Kweon, K. B. Kwon, J. W. Park, T. R. Yoon, and B. H. Park. 2009. Inhibition of IL-1beta-mediated inflammatory responses by the IkappaB alpha super-repressor in human fibroblast-like synoviocytes. *Biochem. Biophys. Res. Commun.* 378: 90–94.
54. Madorin, W. S., T. Rui, N. Sugimoto, O. Handa, G. Cepinskas, and P. R. Kvietys. 2004. Cardiac myocytes activated by septic plasma promote neutrophil transendothelial migration: role of platelet-activating factor and the chemokines LIX and KC. *Circ. Res.* 94: 944–951.
55. Wuyts, A., S. Struyf, K. Gijsbers, E. Schutyser, W. Put, R. Conings, J. P. Lenaerts, K. Geboes, G. Opdenakker, P. Menten, et al. 2003. The CXC chemokine GCP-2/CXCL6 is predominantly induced in mesenchymal cells by interleukin-1beta and is down-regulated by interferon-gamma: comparison with interleukin-8/CXCL8. *Lab. Invest.* 83: 23–34.
56. Schnyder-Candrian, S., R. M. Strieter, S. L. Kunkel, and A. Walz. 1995. Interferon-alpha and interferon-gamma down-regulate the production of interleukin-8 and ENA-78 in human monocytes. *J. Leukoc. Biol.* 57: 929–935.
57. Duchene, J., F. Lecomte, S. Ahmed, C. Cayla, J. Pesquero, M. Bader, M. Perretti, and A. Ahluwalia. 2007. A novel inflammatory pathway involved in leukocyte recruitment: role for the kinin B1 receptor and the chemokine CXCL5. *J. Immunol.* 179: 4849–4856.
58. Lemos, H. P., R. Grespan, S. M. Vieira, T. M. Cunha, W. A. Verri, Jr., K. S. Fernandes, F. O. Souto, I. B. McInnes, S. H. Ferreira, F. Y. Liew, and F. Q. Cunha. 2009. Prostaglandin mediates IL-23/IL-17-induced neutrophil migration in inflammation by inhibiting IL-12 and IFNgamma production. *Proc. Natl. Acad. Sci. USA* 106: 5954–5959.
59. Horai, R., M. Asano, K. Sudo, H. Kanuka, M. Suzuki, M. Nishihara, M. Takahashi, and Y. Iwakura. 1998. Production of mice deficient in genes for interleukin (IL)-1alpha, IL-1beta, IL-1alpha/beta, and IL-1 receptor antagonist shows that IL-1beta is crucial in turpentine-induced fever development and glucocorticoid secretion. *J. Exp. Med.* 187: 1463–1475.
60. Zheng, H., D. Fletcher, W. Kozak, M. Jiang, K. J. Hofmann, C. A. Conn, D. Soszynski, C. Grabiec, M. E. Trumbauer, A. Shaw, et al. 1995. Resistance to fever induction and impaired acute-phase response in interleukin-1 beta-deficient mice. *Immunity* 3: 9–19.
61. Johnston, B., A. R. Burns, M. Suematsu, T. B. Issekutz, R. C. Woodman, and P. Kubes. 1999. Chronic inflammation upregulates chemokine receptors and induces neutrophil migration to monocyte chemoattractant protein-1. *J. Clin. Invest.* 103: 1269–1276.
62. Furie, M. B., and D. D. McHugh. 1989. Migration of neutrophils across endothelial monolayers is stimulated by treatment of the monolayers with interleukin-1 or tumor necrosis factor-alpha. *J. Immunol.* 143: 3309–3317.
63. Denny, M. F., S. Yalavarthi, W. Zhao, S. G. Thacker, M. Anderson, A. R. Sandy, W. J. McCune, and M. J. Kaplan. 2010. A distinct subset of proinflammatory neutrophils isolated from patients with systemic lupus erythematosus induces vascular damage and synthesizes type I IFNs. *J. Immunol.* 184: 3284–3297.

Current Immunology Reviews, 2012, *8*, 12-22

Dendritic Cells in Hepatitis Virus Infection: A Legatus Within

Tatsuya Kanto*

Department of Gastroenterology and Hepatology and Department of Dendritic Cell Biology and Clinical Applications, Osaka University Graduate School of Medicine, Osaka 565-0871, Japan

Abstract: Hepatitis B or C virus (HBV or HCV) causes chronic liver diseases that eventually progress to liver cancer. Both viruses are armed with multiple machineries for modulating immune responses in infected hosts. Mild and pervasive immune cell dysfunction, but not fully compromised, is a hallmark of chronic HBV or HCV infection, of which fundamental mechanisms are yet to be clarified. Dendritic cells (DC) as immune sentinels sense virus *via* toll-like receptors (TLR) or retinoic acid inducible gene-I (RIG-I) and evoke a cascade of immune reactions by secreting cytokines or by interacting other lymphocytes. Reduced and disabled DC potentially give negative impact on adjacent cells, such as NK cells, NKT cells and T cells. However, lack of evidence for active viral replication in DC or blood cells imply the presence of undisclosed contrivances that are independent of infection. Successful treatment of chronically infected patients with anti-viral agents is accompanied with numerical and/or functional restoration of DC, suggesting that DC could serve as potential therapeutic targets. Further studies are warranted for the establishment of therapeutic DC vaccine in order to gain more vigorous and sustained virus-specific immune responses. Cross talk between DC and lymphocytes are thus critical in shaping innate and subsequent adaptive immune responses against hepatitis virus, either spontaneously or therapeutically.

Keywords: Dendritic cells, HBV, HCV, interferon, natural killer cells, natural killer T cells.

INTRODUCTION

Hepatitis B virus (HBV) and hepatitis C virus (HCV) are two major causes of chronic liver disease worldwide. HBV is a small DNA virus that is a prototype of *Hepadnaviridae* family, while HCV is s single stranded RNA virus that belongs to *Flaviviridae*. Both viruses are hepatotrophic, but not directly cytopathic and elicit progressive liver injuries resulting in end-stage liver disease unless effectively eradicated [1, 2]. Epidemiological studies revealed that the relative percentages of acutely infected patients developing chronic hepatitis are different when comparing HBV and HCV infection. Less than 10% of HBV-infected patients develop chronic hepatitis, while more than 80% of HCV-infected ones do so [1, 2]. Such difference may in part rely on the differences in the immunogenicity of viral proteins and the kinetics of viral replication during the early stages of infection [3]. One of the major determinants in the clinical course of viral hepatitis is the host immune response. It has been proposed that the ability of infected hosts to mount a vigorous and sustained cellular immune reactions to HBV and HCV is required for control in primary infection. Once HBV or HCV survives the initial interaction with the host immune system, it uses several means to nullify the selective immunological pressure during the later phases of infection. First, these viruses alter their antigenic epitopes recognized by T cells and neutralizing antibodies to escape immune surveillance [4, 5]. HBV and HCV also subvert immune functions, including those of NK cells, dendritic cells (DC) and T cells. Antiviral agents, pegylated interferon (IFN)-α, ribavirin and nucleot(s)ide analogues, widely used for the treatment of chronic HBV or HCV infection reduce the viral load or enhance immunity in order to prevent the subsequent development of liver cirrhosis or hepatocellular carcinoma (HCC) [1, 6].

Cumulative reports have shown that innate immune system dictates the direction and magnitude of subsequent adaptive immune response. It is generally accepted that HBV- or HCV-specific $CD8^+$ T cells are responsible for virus elimination by inducing hepatocyte apoptosis [4, 5]. Innate immune cells, including NK cells and NKT cells, may contribute to HBV or HCV eradication after primary infection; however, their roles in chronically infected state remain elusive. Since dendritic cells (DC) orchestrate anti-viral immune response by linking innate and adaptive arms of immune system [7], functional impairment of DC leads to failure of NK cells, NKT cells, $CD4^+$ and $CD8^+$ T cells. Infiltration of disabled $CD8^+$ T cells to the infected liver may result in weak liver inflammation that is not sufficient for HBV or HCV eradication [8].

In this paper, we discuss the current understandings of the roles of innate and adaptive immunity in the pathogenesis of hepatitis virus infection as well as efficacy of anti-viral therapy, especially focused on interaction of DC and other players.

KEY PLAYERS IN IMMUNE RESPONSES TO VIRAL HEPATITIS

After HBV or HCV infects the liver, viral replication continues and viral particles are continuously released into the circulation. Theoretically, the first lines of defense are provided by anti-viral type I IFN and subsequent IFN-inducible genes (ISGs). As for cellular components in innate immune system, NK and NKT cells play major roles in liver

*Address correspondence to this author at the Department of Gastroenterology and Hepatology and Department of Dendritic cell Biology and Clinical Applications, Osaka University Graduate School of Medicine, 2-2 Yamada-oka, Suita, Osaka 565-0871, Japan; Tel: +81-6-6879-3446; Fax: +81-6-6879-3448; E-mail: kantot@gh.med.osaka-u.ac.jp

1875-631X/12 $58.00+.00

immunology, of which populations are relatively increased in the liver compared to the periphery. These cells are activated in the liver, where expression of IFN-α and ISGs are extremely high during the early phase of hepatitis virus infection [9]. Activated NK and NKT cells secrete IFN-γ, which inhibits replication of hepatitis virus mainly through a non-cytolytic mechanism (Fig. **1a**) [10].

Dendritic cells (DC) or resident macrophages in the liver are capable of taking up viral antigens, and processing and presenting them to other immune cells (Fig. **1b**) [7]. Since DC express distinct sets of toll-like receptors (TLRs) and cytosolic pathogen sensors [11], it is likely that some viral components stimulate DC through ligation of these receptors (Fig. **2**). DC develop a mature phenotype and migrate to lymphoid tissues (Fig. **1c**), where they stimulate effectors, including T cells and B cells (Fig. **1d**). Following the encounter of DC with other cells, DC secrete various cytokines (IL-12, TNF-α, IFN-α and IL-10) instructing or regulating the functions of the adjacent cells [7]. In addition to these cytokines, DC express various co-stimulatory molecules and ligands to enhance or limit the functions of immune and infected cells. The existence of functionally and ontogenetically distinct DC subsets has been reported; i.e., myeloid DC (MDC) and plasmacytoid DC (PDC) [12]. MDC predominantly produce IL-12 or TNF-α following pro-inflammatory stimuli, while PDC release a considerable amount of IFN-α upon virus infection depending on the immune stimulus; both cytokines in actuality can be made by both cells. Helper T cells have an immunoregulatory function mediated by the secretion of cytokines that support either cytotoxic T lymphocyte (CTLs) generation (Th1 with secretion of IL-2, IFN-γ and TNF-α) or B cell function and antibody production (Th2 with secretion of IL-4, IL-5, IL-10 and IL-13) (Fig. **1e**). In addition to Th1/Th2 paradigm, $CD4^+$ T cells secreting IL-17 (Th17) are induced under distinct cytokine conditioning and are involved in liver inflammation or autoimmunity. DC ontogeny and DC-derived cytokines are crucially associated with the differentiation or polarization of helper T cell subsets.

It is generally accepted that adaptive immunity performs a critical role during the clinical courses of hepatitis. The involvement of antigen-specific $CD4^+$ T cells in HBV or HCV eradication has been well described during both acute or chronic infection [5]. However, there is little evidence that $CD4^+$ T cells mediate direct liver cell injury in virus infection. Thus, it is likely that $CD4^+$ T cells play a critical role in facilitating other antiviral immune mechanisms, such as enhancing $CD8^+$ effector function. The antigen-primed CTLs recruit to the liver (Fig. **1f**) and constitute the critical element in the eradication of virus-infected cells (Fig. **1g**). The increment of specialized immune suppressors such as regulatory T cells (Tregs) has been shown in HBV or HCV infection [13, 14]. These cells are actively involved in the alleviation of Th1- or CTL-mediated liver inflammation, thus contributing to persistence of hepatitis virus (Fig. **1h**).

NATURAL COURSE OF ACUTE HBV OR HCV INFECTION

Acute HBV Infection

During the early phase of primary HBV infection, HBV-DNA is not detectable in serum or the liver for 4-7 weeks following exposure. HBV infection of the liver directly induces type I IFN, which subsequently activates NK cells. Thus, even in the incubation phase, activated NK cells are thought to play crucial role in the control of HBV replication by producing IFN-γ. This is supported by the observation that circulating NK cells increases before the peak of HBV replication, which subsides following HBV reduction [15]. Activated NKT cells are involved in the inhibition of HBV replication, as evidenced by

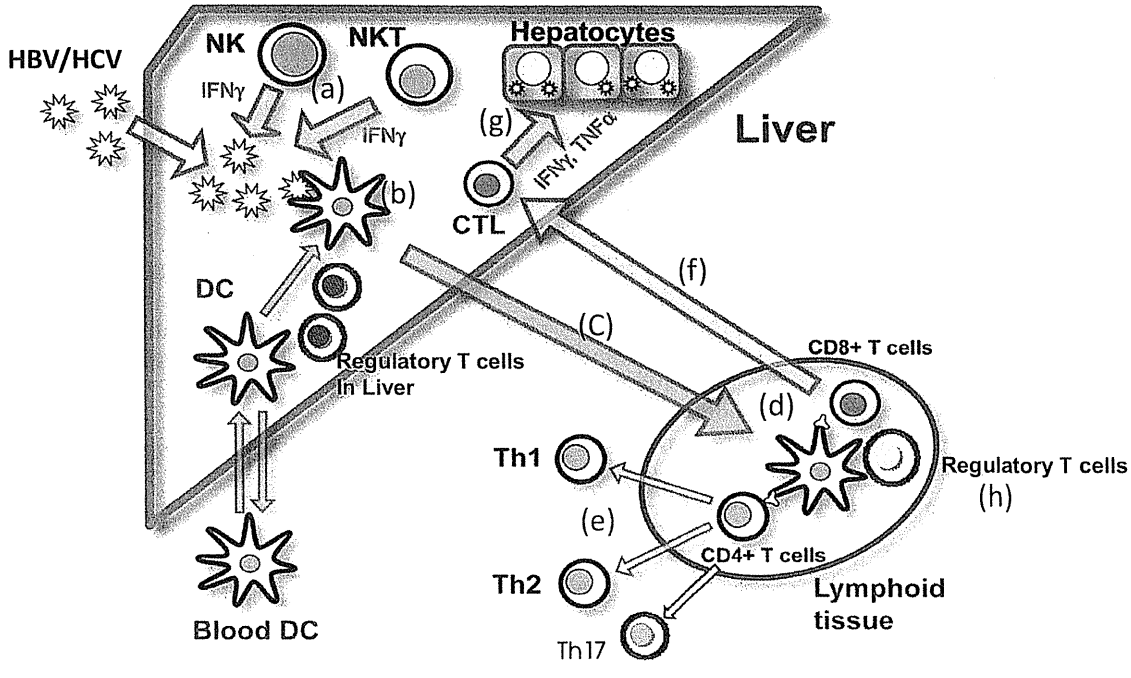

Fig. (1). Key players in immune reactions in viral hepatitis. CTL, cytotoxic T lymphocyte; DC, dendritic cell; HBV, hepatitis B virus; HCV, hepatitis C virus; NK, natural killer cell; NKT, natural killer T cell; Th, helper T cell. (**a**)-(**h**), see text.

HBV transgenic mouse model [16]. Increment of human NT cells, as defined as $CD3^+CD56^+$ cells, is observed in acute hepatitis B prior to the peak of T cell responses [17]. Subsequently a rapid increase in HBV replication occurs at 10-12 weeks of infection, which is accompanied by induction of adaptive immunity. HBV-specific $CD4^+$ and $CD8^+$ T cells are detectable in the blood even before the onset of overt hepatitis [15]. In chimpanzee inoculated with a single strain of HBV, the size of viral burden may be one of the determinants dictating the outcomes. The larger size of HBV is administered, the higher chance of immune-mediated HBV clearance is gained in chimpanzees [18]. Generally, strong and Th1-biased $CD4^+$ T cell response and multi-specific $CD8^+$ response are associated with HBV clearance [19]. HBV-specific $CD8^+$ T cells continue to increase after a marked reduction in HBV-DNA and reach their highest number at the time of maximal ALT levels (0.1-1.3% of peripheral $CD8^+$ T cells), then decline during the recovery phase, in parallel with a resolution of hepatitis [15, 19]. From a $CD4^+$- or $CD8^+$ T cell depletion study in chimpanzees, HBV-specific $CD8^+$ T cells, but not $CD4^+$, are the main effectors responsible for viral clearance [20]. In comparison with HCV-specific $CD8^+$ T cells using tetramers, HBV-specific $CD8^+$ T cells are highly activated and capable of proliferating and secreting much IFN-γ [21]. Since interactions among IFN, NK and T cells seem to be complicated in the acute phase, suppressive factors are involved as a compensatory mechanism. In this context, HBV-induced IL-10 at primary infection may be closely related with down-regulation of $CD4^+$ and $CD8^+$ T cell responses [22].

Acute HCV Infection

In clear contrast with HBV, HCV-RNA levels rapidly increase during the first few days of HCV infection and continue to be high during the incubation periods [23], which lasts for up to 10-12 weeks following infection. Although HCV triggers expression of type I IFN and ISGs in liver during this phase [9], the HCV viral load does not decrease. This suggests that HCV impedes the execution of anti-viral molecular mechanisms, including interferon regulatory factor (IRF)-3 [24], as well as NF-κB and RNA-dependent protein kinase (PKR) [25]. In parallel with the onset of acute hepatitis, activated HCV-specific T cells enter the liver [26]. HCV-specific $CD4^+$ and $CD8^+$ T-cell responses and IFN-γ co-expression coincide with decreases in HCV quantity [26]. Vigorous, multi epitope-specific, Th1 type and sustained $CD4^+$ T cell responses are detected in resolved cases [23]. By contrast, in cases that progress to chronic hepatitis, $CD4^+$ T cell responses are weak, narrowly selected and short-lived [27]. The frequency of HCV-specific $CD8^+$ T cells is high during the acute phase of infection (2-8% of peripheral $CD8^+$ T cells), however, it decreases after HCV persistence develops (0.01-1.2%) [28]. Despite the high numbers of CTL, some of these cells are "stunned" in acute phase, as demonstrated by an inability to produce IFN-γ and to proliferate in response to HCV antigens [28, 29].

INNATE IMMUNITY

Interferon and Interferon-Stimulated Genes

Mammalian toll-like receptors (TLRs) sense some pathogen-associated molecular patterns (PAMP) embedded in virus components and then induce inflammatory cytokines or type-I IFN, resulting in the augmentation of anti-virus immune reactions [11]. Retinoic acid inducible gene-I (RIG-I) and melanoma differentiation antigen (MDA) -5 are cytosolic molecule that sense dsRNA as virus replicative intermediate, which subsequently activates IRF-3 and NF-κB pathways [30]. Several lines of evidence have been presented that HBV or HCV impedes TLR- or RIG-I-dependent signal transduction, resulting in lesser magnitude of ISG responses.

HBV Infection

Limited information is available for which HBV components stimulate relevant PAMP receptors. In general, activation of TLR-dependent pathways suppresses HBV replication both *in vitro* and *in vivo* [31]. In chronic HBeAg-positive patients, it is reported that TLR2 expression is down-regulated in hepatocytes, Kupffer cells or monocytes, suggesting that TLR2-dependent pathway in these cells is impaired [32]. Acute-on-chronic hepatitis B is a critical liver disease that frequently becomes fatal. In such patients who failed to survive, the expression of TLR3 and IFN-β in monocyte-derived DC (MoDC) was significantly decreased compared to those who survived.[33]. These results suggest that TLR3-dependent pathways are involved in either a cause or a consequence of liver inflammation. In mice, HBs, HBe antigens and HBV virions are capable of inhibiting TLR-dependent pathways [34]. Recently, it has been shown that HBV-X protein directly degrade adaptor molecule MAVS, resulting in the inhibition of RIG-I-dependent signaling pathways [35]. Alternatively, Yu *et al.* reported that, in the shared downstream of TLR and RIG-I, HBV polymerase is responsible for IRF3 inhibition at the levels of TBK1/IKKε [36].

HCV Infection

Large-scale cohort study on US veterans revealed that the prevalence of various infectious diseases, including virus, bacteria and parasites, in HCV-infected individuals is significantly higher than those in uninfected controls [37]. These observations suggest that first-line defense against pathogens, of which system is initiated by TLR/RIG-I stimulation, is functionally impaired in HCV infection. Several mechanisms have been proposed regarding to HCV-induced suppression of innate immunity. By using HCV subgenomic replicon system, it has been demonstrated that HCV NS3/4A proteins influences on the functions of adaptor molecules mediating TLR-dependent and RIG-I-dependent pathways, resulting in an impairment of the induction of IFN-β as well as subsequent ISGs [38, 39]. However, it is yet to be proven whether the results obtained from HCV replicon are applicable or not for HCV-infected individuals. HCV core has been reported as one of the crucial immunogenic components. Several molecules have been regarded as targets of HCV core-mediated immune alteration, such as STAT1 [40] or SOCS3 [41], all of which eventually dampen IFN and ISG induction. Alternatively, in mouse macrophage cell line, HCV NS5A is shown to inhibit TLR-dependent IFN response by interacting adaptor molecule, MyD88 [42].

To investigate the roles of TLR/RIG-I in HCV infection, we compared their expressions and the functions in MDC and PDC between the patients and donors. In MDC from HCV-infected patients, TLR2, TLR4 and RIG-I expression were significantly higher than those in healthy counterparts [43]. Of particular interest, regardless of the higher expressions, specific agonists for these sensors stimulated patients MDC to induce lesser amount of IFN-β and TNF-α compared to donor MDC [43]. These results show that, in MDC, the signal transduction *via* these receptors is strongly impeded in HCV infection. Further investigation is needed to clarify which TLR or RIG-I is predominantly utilized by HCV to evoke immune reactions.

Natural Killer Cells

Within the liver, NK cells comprise 20-30% of mononuclear cells, as compared to that they consist of 10-15% in PBMC [44]. It thus needs to be stressed that such regional differences in the distribution of NK cells may raise conflicting analytical results of these cells. In HBV- or HCV-infected liver, NK cells are deemed to be activated by type-I IFN and have gained ability to produce substantial amount of IFN-γ. Recently, it is reported that such NK activation at this phase is not always correlated with the outcomes of infection, but they are capable of dictating further T cell responses [45, 46]. Cumulative data have shown that activated NK cells, not only T cells, could be effectors in liver injury in HBV or HCV infection, in which TRAIL-mediated apoptosis is involved.

Natural Killer cells express various functional receptors; the one group that transduces inhibitory signals (Killer Inhibitory Receptors/KIRs, CD94, NKG2A) and the other does activating signals (NKG2D). The function of NK cells is dynamically regulated *in vivo* by the balance between expressions of counteracting receptors and their association with relevant ligands [47]. Large scale cohort studies in HCV infection have disclosed that certain combinations of HLA-C and KIR haplotypes are closely associated with spontaneous HCV clearance [48, 49]. Such epidemiological observations raise a possibility that NK cells play an active role in HCV eradication.

We compared the expressions of NK cell receptor between HCV-infected patients and healthy donors. As for inhibitory receptors, KIR expressions are not different between the groups; however, CD94 and NKG2A expressions are higher in patients than controls [50]. In contrast, activating receptor NKG2D expression is comparable between the groups. It is yet to be determined how the expression of NK cell receptor is regulated. In our hands, HCV pseudo-virus did not enter purified NK cells, suggesting that NK cells are not susceptible to direct HCV infection (unpublished data). Thus, some soluble factors and/or direct binding of HCV particles to NK cells might be the cause of NK receptor dysregulation.

Natural Killer T Cells

Natural killer T (NKT) cells are a unique lymphocyte subset co-expressing T-cell receptor (TCR) and NK cell markers [51]. The NKT cell population is highly heterogeneous according to the differences in types and tissue distribution; invariant (or classical) NKT (iNKT) cells express an invariant TCR, composed of Vα24-JαQ preferentially paired with Vβ11 in humans [51], whereas non-invariant NKT cells express diverse TCR. Invariant NKT cells recognize glycolipid antigens presented on CD1d expressed by DCs [51]. Although endogenous ligands of iNKT cells are little known, α-galactosyl-ceramide (αGalCer) has been used as a surrogate for natural ligands. In contrast, non-invariant NKT cells are activated by CD1d-dependent manner but are not reactive to αGalCer. Baron *et al.* reported that, in HBV-transgenic mice, non-invariant NKT cells are critically involved in acute liver injury [52]. As for a human counterpart, Exley *et al.* observed that CD1d-restricted non-invariant NKT cells are infiltrated in HCV-infected liver, where they presumably exert their promoting role in liver inflammation [53]. Hepatic inflammatory cells or biliary cells up-regulate CD1d expression which subsequently supports NKT cell activation [54]. In addition, hepatic stellate cells are capable of activating NKT cells *via* surface CD1d and secretion of IL-15 [55].

For chronic HCV infection, some controversial reports have been published about the frequency of iNKT cells [56, 57], however, their functional roles in HCV-infected patients are largely unknown. We demonstrate that the number and functions of iNKT cells from HCV-infected patients are comparable with those from healthy subjects at the steady state [58]. By contrast, activated iNKT cells from patients released more Th2 cytokines, most significantly IL-13, than those from the controls [58]. Recently, other groups have reported that IL-4 and IL-13 from fresh iNKT cells were increased in liver cirrhosis caused by HBV or HCV, implying that these cells are pro-fibrogenic to the liver [59]. If this is the case, our findings suggest that iNKT cells in chronic HCV infection are pro-fibrogenic per se even in the pre-cirrhotic stage. The reason why iNKT cells in HCV infection are Th2-biased needs to be further investigated.

Dendritic Cells

HBV Infection

Several reports have been available for functional alterations of DC subsets in HBV infection [60]. Infection of HBV to DC is still controversial and the described functional defects are minimal when compared with HCV [61, 62]. It is reported that peripheral PDC are phenotypically and functionally intact [63]. In contrast, PDC ability of secreting IFN-α is reported to be impaired specifically in response to TLR9 but not to TLR7 agonists [64]. As for the mechanisms, HBs antigen is responsible for such PDC disability partly by up-regulating suppressor molecule SOCS-1 [64]. Similarly, other investigators reported that PDC frequency as well as their TLR9 expression are decreased [65]. In addition to PDC, MDC dysfunction is observed as well, which is presumably caused by HBV particles and HBs antigen [66].

In contrast to circulating PDC, liver-infiltrating counterparts are more vulnerable to HBV; liver PDC are significantly reduced and disabled in non-survivors of acute-on-chronic hepatitis B compared to those in survivors [67]. Blockade of PDC-derived IFN-α downgraded the amounts of IL-12 and TNF-α released from adjacent cells [67],